Digital Comprehensive Summaries of Uppsala Dissertations
from the Faculty of Pharmacy 364

Translational Aspects of Brain-Specific Drug Delivery by Targeting Active Uptake at Brain Barriers

FRIDA BÄLLGREN

ACTA UNIVERSITATIS
UPSALIENSIS
2024

ISSN 1651-6192
ISBN 978-91-513-2289-6
urn:nbn:se:uu:diva-540918

UPPSALA
UNIVERSITET

Dissertation presented at Uppsala University to be publicly examined in room A1:111a, Biomedicinskt Centrum (BMC), Husargatan 3, Uppsala, Friday, 13 December 2024 at 09:15 for the degree of Doctor of Philosophy (Faculty of Pharmacy). The examination will be conducted in English. Faculty examiner: Professor Joseph Nicolazzo (Faculty of Pharmacy and Pharmaceutical Sciences, Monash University, Australia).

Abstract
Bällgren, F. 2024. Translational Aspects of Brain-Specific Drug Delivery by Targeting Active Uptake at Brain Barriers. *Digital Comprehensive Summaries of Uppsala Dissertations from the Faculty of Pharmacy* 364. 76 pp. Uppsala: Acta Universitatis Upsaliensis.
ISBN 978-91-513-2289-6.

Challenges in central nervous system (CNS) drug development often arise from difficulties in achieving safe and effective brain drug delivery. Key to addressing this issue is ensuring sufficient drug concentrations at the CNS target site. This requires efficient drug transport across brain barriers and reliable translation of preclinical findings to clinical settings. The proton-coupled organic cation (H^+/OC) antiporter, associated with blood-brain barrier (BBB) uptake of several marketed CNS drugs, has emerged as a promising target in this regard. However, several critical questions are unresolved for fully leveraging this system in drug development. The studies in this thesis investigated key translational pharmacokinetic questions of the CNS delivery of antiporter substrates. This included characterization of the uptake across several CNS barriers, potential sex and species differences, the impact of inflammation, *in vitro-in vivo* correlations, and regional CNS distribution. Oxycodone served as the primary model substrate across *in vitro* and *in vivo* studies, including microdialysis, the Combinatory Mapping Approach for Regions of Interest, and *in vitro* BBB cell models. Active uptake was confirmed at the BBB and revealed at the blood-cerebrospinal fluid barrier (BCSFB) and blood-spinal cord barrier in rats. Novel evidence of active uptake at the pig BBB and BCSFB was presented, suggesting potential translatability to humans. Cerebrospinal fluid, often used as a proxy for brain concentrations in the clinic, underestimated antiporter substrate exposure, necessitating caution in its use as a surrogate for brain interstitial fluid. Importantly, no sex-related differences were observed in BBB uptake, supporting the antiporter as a viable target in CNS drug development. Lipopolysaccharide-induced inflammation significantly reduced the uptake. Although the active uptake was reduced, net uptake was still present during inflammation. *In vitro* BBB models of various origins (mouse, rat, pig, human) reflected *in vivo* findings, supporting the utility of these models for verification of active uptake. A consistent net uptake, with minor regional differences, was observed in the CNS delivery of antiporter substrates. These findings contribute to advancing CNS drug development by highlighting the significance of active uptake transporters and the necessity for comprehensive neuropharmacokinetic evaluations both *in vitro* and *in vivo*.

Keywords: Pharmacokinetics, Brain drug delivery, Blood-brain barrier, Blood-cerebrospinal fluid barrier, Blood-spinal cord barrier, Proton-coupled organic cation antiporter, Oxycodone, Microdialysis, Rat, Pig, Lipopolysaccharide-induced inflammation, Neurotoxicity, hCMEC/D3, Primary brain endothelial cells

Frida Bällgren, Department of Pharmacy, Box 580, Uppsala University, SE-75123 Uppsala, Sweden.

ISSN 1651-6192
ISBN 978-91-513-2289-6
URN urn:nbn:se:uu:diva-540918 (http://urn.kb.se/resolve?urn=urn:nbn:se:uu:diva-540918)

To all of you who supported me during this journey!

List of Papers

This thesis is based on the following papers, referred to in the text by their Roman numerals.

I. **Bällgren, F.**, Hammarlund-Udenaes, M., Loryan, I. (2023) Active Uptake of Oxycodone at Both the Blood-Cerebrospinal Fluid Barrier and The Blood-Brain Barrier without Sex Differences: A Rat Microdialysis Study. *Pharm Res*, 40(11):2715-2730. Doi: 10.1007/s11095-023-03583-0

II. **Bällgren, F.**, Hammarlund-Udenaes, M., Loryan, I. (2024) Reduced Oxycodone Brain Delivery in Rats Due to Lipopolysaccharide-Induced Inflammation: Microdialysis Insights into Brain Disposition and Sex-Specific PK. *Fluids Barriers CNS. Submitted.*

III. **Bällgren, F.**, Bergfast, T., Ginosyan, A., Mahajan, J., Lipcsey, M., Hammarlund-Udenaes, M., Syvänen, S. and Loryan, I. (2024) Active CNS Delivery of Oxycodone in Healthy and Endotoxemic Pigs. *Fluids Barriers CNS,* 21, 86. Doi: 10.1186/s12987-024-00583-z

IV. **Bällgren, F.**, Svane, N., Ginosyan, A., Bay Villekjær Pedersen, A., Li, S., Mahajan, J., Hammarlund-Udenaes, M., Brodin, B., and Loryan, I. Comparative analysis of the uptake of H^+/OC antiporter substrates oxycodone and pyrilamine across and into brain endothelial and parenchymal cells. *Manuscript.*

V. **Bällgren, F.**, Hu, Y., Li, S., van de Beek, L., Hammarlund-Udenaes, M. and Loryan, I. (2024) Region-Independent Active CNS Net Uptake of Marketed H^+/OC Antiporter System Substrates. *Front Cell Neurosci.* Doi: 10.3389/fncel.2024.1493644

Reprints were made with permission from the respective publishers.

Related publications

Hu, Y., Girdenyté, M., Roest, L., Liukkonen, I., Siskou, M., **Bällgren F.,** Hammarlund-Udenaes, M., Loryan, I. (2024) Analysis of the contributing role of drug transport across biological barriers in the development and treatment of chemotherapy-induced peripheral neuropathy. *Fluids Barriers CNS*, 8;21(1):13. Doi: 10.1186/s12987-024-00519-7

Svane, N., **Bällgren, F.**, Ginosyan, A., Kristensen, M., Brodin, B. and Loryan, I. (2024) Regional distribution of unbound eletriptan and sumatriptan in the CNS and PNS in rats: Implications for a potential central action. *J Headache Pain. Accepted.*

Contents

Abbreviations

aECF	Artificial extracellular fluid
AUC	Area under the concentration-time curve
BBB	Blood-brain barrier
BCSFB	Blood-cerebrospinal fluid barrier
BEC	Brain endothelial cells
BSCB	Blood-spinal cord barrier
CMA	Combinatory Mapping Approach
CNS	Central nervous system
CSF	Cerebrospinal fluid
$C_{tot,plasma,ss}$	Total plasma concentration at steady-state
$C_{u,plasma,ss}$	Unbound plasma concentration at steady-state
ΔC	Difference in concentration
DIS	Drug-induced seizures
DMEM	Dulbecco's Modified Eagle's Medium
ER	Efflux Ratio
f_u	Fraction of unbound drug
$f_{u,brain}$	Fraction of unbound drug in the brain
$f_{u,cell}$	Fraction of unbound drug in the cell
$f_{u,D}$	Unbound buffer-to-diluted tissue concentration ratio
$f_{u,plasma}$	Fraction of unbound drug in plasma
$f_{u,ROI}$	Fraction of unbound drug in brain region of interest
hCMEC/D3	Immortalized Human Cerebral Microvascular Endothelial Cell line
IC_{50}	Half-maximal inhibitory concentration
IL	Interleukin
ISF	Interstitial fluid
K_m	Michaelis Constant
$K_{p,brain}$	Total brain-to-plasma concentration ratio
$K_{p,CSF}$	Total CSF-to-plasma concentration ratio
$K_{p,ROI}$	Total brain region-to-plasma concentration ratio
$K_{p,u,cell}$	Total cell-to-unbound buffer concentration ratio
$K_{p,uu}$	Unbound partition coefficient
$K_{p,uu,brain}$	Unbound brain-to-plasma concentration ratio
$K_{p,uu,cell}$	Unbound intracellular-to-extracellular concentration ratio
$K_{p,uu,CSF}$	Unbound CSF-to-plasma concentration ratio
$K_{p,uu,lumbarCSF}$	Unbound lumbar CSF-to-plasma concentration ratio

$K_{p,uu,LV}$	Unbound lateral ventricular CSF-to-plasma concentration ratio
$K_{p,uu,ROI}$	Unbound brain region-to-plasma concentration ratio
LHFPL6	LHFPL tetraspan subfamily member 6
LPS	Lipopolysaccharide
MCAE	Mood- and cognitive-related adverse event
MS/MS	Tandem mass spectrometry
OCT	Organic cation transporter
PBS	Phosphate-buffered saline
PCA	Principal Component Analysis
PD	Pharmacodynamics
P-gp	P-glycoprotein
PK	Pharmacokinetics
ROI	Region of interest
SLC	Solute carrier
SOFA	Sequential Organ Failure Assessment
TEER	Transendothelial electrical resistance
TM7SF3	TransMembrane 7 SuperFamily member 3
TNF–α	Tumor necrosis factor-alpha
TRITC	Tetramethyl-rhodamine B isothiocyanate
UPLC	Ultra-Performance Liquid Chromatography
$V_{u,brain}$	Unbound drug volume of distribution in the brain

Introduction

There is an urgent need to treat diseases affecting the central nervous system (CNS). Thousands of compounds are screened on a yearly basis in an attempt to identify potential novel CNS drug candidates. However, despite all efforts, CNS candidates have had a lower success rate during development than those for non-CNS indications[1-3]. A combination of factors associated with pharmacodynamics (PD), pharmacokinetics (PK), and translational aspects, including translating preclinical research findings to a successful clinical drug candidate, have been identified to be responsible for the low success rate[4, 5]. One of the key reasons for failure is inadequate CNS exposure due to the protective functions of the CNS barriers[6]. In this regard, active uptake transporters, such as the putative proton-coupled organic cation (H^+/OC) antiporter system – which is associated with the active uptake of several marketed drugs across the blood-brain barrier (BBB) – have high potential to be investigated as brain drug delivery targets. Despite the two decades of ongoing research investigations, several key translational PK questions remain unanswered and limit the drug discovery and development of novel CNS drug candidates utilizing this system. This includes characterization of uptake across other CNS barriers, translation between health and disease conditions in rats and higher species, between *in vitro* and *in vivo* findings, potential sex-dependent differences in brain drug delivery, as well as safety concerns. These PK-related factors are the key focus areas in this thesis.

The CNS

The CNS consists of the brain and the spinal cord. The brain contains an extensive capillary network that supplies it with blood, ensuring that all neurons are located within approximately 25 µm of a capillary[7]. From a neuropharmacokinetic (neuroPK) point of view, it is essential to understand the impact of fluid and barrier dynamics on drug CNS exposure in health and disease. On this point, both cerebrospinal fluid (CSF) and interstitial fluid (ISF) are investigated to assess drug concentrations.

Barriers of the CNS

The barriers of the CNS refer to the cellular barriers present at the interfaces between blood and brain, CSF, and spinal cord (Figure 1). These barriers maintain the CNS homeostasis and protect the brain and spinal cord by regulating the transport of ions and molecules into and out of the CNS, with restrictive functions such as tight junctions and efflux transporters[6]. These interfaces between blood and the CNS are dynamic and respond to signals from both the blood and the CNS[8]. Two main brain barriers are the BBB and the blood-CSF barrier (BCSFB) controlling the composition of brain ISF and CSF, respectively[7, 9, 10]. The BBB, composed of brain capillary endothelial cells, is extensively studied due to its large surface area, which facilitates the exchange of a variety of compounds, including essential nutrients (e.g., glucose and amino acids), endogenous molecules (e.g., hormones), metabolic waste products, and therapeutic agents between the blood and the brain[11]. Due to its large surface area and a short distance to neurons, the BBB is considered to have a predominant role in brain microenvironment regulations and is the major path for brain drug delivery[6, 11]. The BCSFB, formed by the choroid plexus epithelium, has a smaller surface area than the BBB and its functions are less studied, but it is still considered to play a role in drug delivery[6, 11]. The blood-spinal cord barrier (BSCB) is anatomically and functionally similar to the BBB. However, there are reported differences between the BSCB and the BBB, such as permeability[12] and extent of drug delivery[13]. For instance, an *in vitro* study demonstrated lower expression levels of tight junctions in endothelial cells from the murine spinal cord compared to those in brain microvascular endothelial cells[14]. The function of the antiporter system has mainly been studied at the BBB and fewer studies are focusing on other CNS barriers, consequently, its function at other CNS barriers is not fully understood.

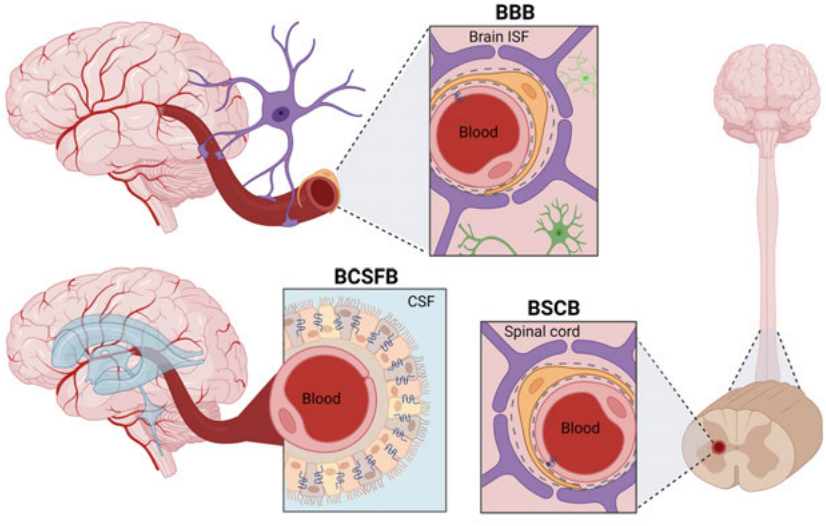

Figure 1. A schematic illustration of the blood-brain barrier (BBB – between the blood and brain interstitial fluid, ISF), blood-cerebrospinal fluid barrier (BCSFB – between blood and brain cerebrospinal fluid, CSF), and blood-spinal cord barrier (BSC – between blood and the spinal cord). The endothelial cells (pink) at the BBB and BSCB are connected with tight junctions and surrounded by pericytes (yellow), basal lamina (dashed lines), and astrocyte end-feet (purple). Other cell types visualized in the brain are neurons (dark green) and microglia (light green). The endothelial cells at the BCSFB are fenestrated, while the barrier consists of choroid plexus cells (light yellow/gray) connected with tight junctions.

Fluids of the CNS

CSF is the fluid surrounding the brain and spinal cord, filling the ventricular spaces, while ISF occupies the extracellular space surrounding the brain's parenchymal cells[15, 16]. The origin of ISF has been studied for over 100 years and there are several possible sources including water produced by brain metabolism, generated by, e.g., oxidation of glucose, and flux across the brain capillary endothelium[15, 17]. The CSF is secreted from the choroid plexus[18-20]. In humans, approximately 500 mL of CSF is secreted per day[18-20]. Also, approximately 20% of CSF has been documented to originate from brain ISF[21, 22]. The CSF has a pulsatile movement throughout the ventricular system driven by arterial pulsations, and changes throughout the day, i.e., related to heart rate, breathing, and circadian rhythm[15, 23-25]. The CNS fluid dynamics involve interactions between ISF and CSF, which is an area that has been extensively studied with several pathways under discussion. The traditional hypothesis includes the production of CSF inside the brain ventricles, circulation

towards subarachnoid space, and drainage to the venous sinuses and the peripheral lymphatic system[26]. The idea of a glia-lymph, "glymphatic", system for waste clearance suggests that CSF enters the brain along arterial pathways and clears ISF along venous routs, with aquaporin-4 expressed at astrocytic end-feet, facilitating convective bulk flow[27]. Also, others have proposed that a perivascular fluid system is of importance for ISF-CSF exchange and waste clearance[22, 28]. However, diffusion is also considered a dominant mechanism of solute transport within the ISF[15]. Neither hypotheses fully explain CNS fluid dynamics, leading to ongoing discussions and highlighting its complexity. CNS fluid dynamics may involve a combination of different mechanisms that are not yet fully understood.

Drug transport at CNS barriers in health and disease

There are different routes of drug transport at brain barriers, including passive transport and carrier-mediated transport via active influx and efflux transporters (Figure 2)[6, 29, 30]. In addition to location and structural differences between CNS barriers, dissimilarities in transporter expression have been reported in animals and humans[6, 31-33]. However, a deeper understanding of drug transport across brain barriers is needed, as limitations in current knowledge have been recognized as a challenge in drug development[34]. The relevance of transporters in drug distribution, elimination, and PK profiles is well accepted and therefore the knowledge of transporter expression and function at different CNS interfaces needs further attention[35]. The brain barriers express efflux transporters, with the key player being the efflux transporter P-glycoprotein (P-gp), but also various active uptake transporters.

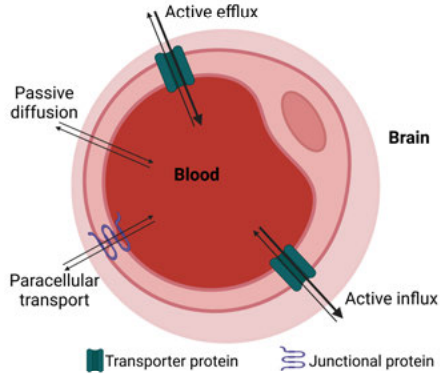

Figure 2. Simplified illustration of brain barrier transport mechanisms. Transcellular transport across endothelial cell membranes can be passive diffusion or active transport. Active transport includes carrier-mediated processes, where transporter proteins facilitate the influx or efflux of molecules into or out of the brain. Paracellular transport between cells is passive and limited at the BBB due to the presence of tight junction proteins between endothelial cells.

Significant changes in the BBB have been documented in disease conditions[6, 36], including CNS diseases[37-41]. These changes include loss of BBB integrity and altered function and expression level of transporters[8, 42-44]. Research on

the impact of disease on BBB transporters has mainly focused on efflux mechanisms, showing that the expression and activity of common efflux transporters, such as P-gp and breast cancer resistance protein, can be altered during conditions such as experimentally induced inflammation[45-47]. In addition to transporter changes, altered CNS fluid dynamics, including impaired CSF flow, have been reported in disease states such as Alzheimer's disease and stroke[48-50]. Both changes regarding transporters and fluid dynamics may affect the CNS exposure of drugs. For example, a study on morphine transport in pigs with meningitis demonstrated an increased drug uptake across the BBB, attributed to a reduction in active efflux and increased paracellular transport[51]. Similarly, in patients with severe brain trauma, morphine transport across the BBB was higher in the damaged brain tissue compared with the tissue on the contralateral side[52]. Despite the clinical importance of understanding such changes, studies on the impact of disease on active uptake transporters remain limited[32]. There have been investigations assessing the impact of inflammation on BBB uptake of H^+/OC antiporter substrates[53, 54]. However, the findings are contradictory, highlighting the complexity and the need for further investigations in this area.

Targeting the proton-coupled organic cation (H^+/OC) antiporter for effective and safe CNS drug delivery

Until now, BBB transport research has mainly been focused on efflux transporters that reduce drug concentrations in the brain[32, 55]. However, to overcome the inadequate CNS exposure of drugs during development, a promising approach is to target active uptake transporters at brain barriers[56, 57]. An example of a system that has been used for CNS drug delivery is the solute carrier (SLC) transporter L-type amino acid transporter 1, which has been used for CNS delivery of several marketed drugs, such as levodopa[58]. Another SLC subfamily of transporters, that is important for CNS drug delivery, is organic cation transporters (OCTs). Since many CNS-active drugs are basic compounds that form cations at physiological pH, this group of transporters is of particular interest. Hence, the multi-substrate H^+/OC antiporter system is a promising target for successful brain drug delivery.

An early study showed carrier-mediated uptake of diphenhydramine at the BBB associated with an unknown active uptake system[59]. After that, several studies demonstrated uptake associated with the same antiporter system[60, 61]. The system was characterized and termed proton-coupled organic cation antiporter as it was assumed to mediate the transport of several cationic drugs[61]. Later, numerous studies on the H^+/OC antiporter function at the BBB, confirming active uptake, have opened up new perspectives for CNS drug delivery[62]. Active BBB uptake associated with the H^+/OC antiporter has been documented for several clinically used CNS drugs both *in vitro* and *in vivo*, such

as oxycodone[63-67], pyrilamine[64-66], diphenhydramine[65, 66, 68], varenicline[69], tramadol[66, 70], bupropion[71], and memantine[53, 66, 72-74]. Antiporter substrates are basic compounds with high pKa values, such as oxycodone with a pKa of 9.1[75], and are therefore also prone to lysosomal trapping[76].

Additionally, the antiporter function has been demonstrated to be driven by an oppositely directed proton gradient[64, 65], with extracellular alkalization or intracellular acidification increasing the uptake *in vitro*[65]. A hypothesis on the endogenous role of the H^+/OC antiporter is, therefore, regulation of brain extra- and intracellular pH. This makes it challenging to determine whether the intracellular accumulation of antiporter substrates is driven by pH partitioning or active uptake at the cell membrane. Moreover, the antiporter activity has been documented to be dependent on substrate concentration and temperature, and independent of extracellular sodium and membrane potential[62]. For the identification of H^+/OC antiporter substrates, pharmacophore models have successfully been developed[77]. Also, two proteins were recently identified to be included in the antiporter system: transmembrane 7 superfamily member 3 (TM7SF3) and LHFPL tetraspan subfamily member 6 (LHFPL6)[78]. Yet, as transporter complexes consisting of multiple proteins are difficult to identify, additional proteins may be involved in the antiporter system, and further investigations are needed[78]. Overall, these findings have widened the possibilities for the design and optimization of new substrates in an attempt to achieve brain-specific drug delivery.

The function of the antiporter system at other CNS barriers than the BBB has so far been sparsely studied. Yet, in the early study, discovering diphenhydramine uptake at the BBB, *in vitro* experiments in isolated rabbit choroid plexus indicated carrier-mediated uptake also at the BCSFB[59]. The extent of antiporter substrate's transport across the rat BBB and BCSFB has been documented[79], and clinical data suggested active uptake at the BCSFB by unbound CSF-to-plasma concentration ratios above unity for antiporter substrates such as bupropion and clozapine[79, 80]. As CSF is often used as a proxy for brain ISF in the clinic, further studies on the H^+/OC antiporter function at the BCSFB are of great importance to evaluate the predictability of CSF.

Potential variations in the CNS drug delivery of antiporter substrates

Sex-dependent differences

A less investigated aspect is transporter function between sexes, as females generally are underrepresented in research[81, 82]. This is the case also for the function of the antiporter system. Potential differences in the function of the antiporter system between sexes may impact not only the PK but also indirectly the PD response. In a clinical study, the analgesic effect of oxycodone was reported to be higher in women compared with that in men[83]. Also, the

oxycodone PK and analgesic effect have been reported to differ between female and male rats, and vary with the estrous cycle, with higher brain oxycodone levels and higher analgesia in females in the diestrus phase[84, 85]. It is not clear if sex-dependent differences in H^+/OC antiporter-mediated barrier transport can explain these observed differences in oxycodone CNS exposure and effect.

Species variations

As animals are often used in preclinical research, such as in the selection of drug candidates prior to clinical trials, the inter-species translation is crucial. Transporter expression level and function may differ between species. For instance, pronounced species differences were found in the function of P-gp at the BBB[86, 87]. The findings have been essential for the interpretation of brain drug delivery when extrapolating preclinical data on P-gp substrates to humans. The H^+/OC antiporter-associated active uptake to the brain has been documented with a similar net active influx in different species[63, 88, 89]. However, its function at the human BBB is not confirmed. To better understand the human BBB in both healthy and disease states, inter-species comparisons of the BBB functions are needed[90]. Bridging data from rodents to higher species, such as pigs, may facilitate the translation to humans.

Correlation between CNS exposure and drug-induced neurotoxicity

CNS drug development often faces high failure rates due to efficacy or safety concerns, particularly CNS neurotoxicity[3, 91]. Drug-induced neurotoxicity, such as drug-induced seizures (DIS), and mood- and cognitive-related adverse events (MCAEs), often goes undetected in preclinical models due to an incomplete understanding of the underlying mechanisms[92], posing a major challenge in the field[93]. Pharmacovigilance data mining has identified drugs linked to DIS and MCAEs[94, 95], particularly those associated with OCTs or the H^+/OC antiporter system[71], resulting in a hypothesis of a connection between antiporter-mediated CNS uptake and drug-induced neurotoxicity. Further, the extent of BBB transport for some of these drugs, including oxycodone, diphenhydramine, and bupropion, has been shown to fluctuate, with significantly higher uptake at early time points after drug administration[63, 68, 96]. This dynamic BBB transport may lead to increased CNS exposure at specific time points, potentially with brain regional specificity, and may contribute to the development of neurotoxicity. Although previous studies have explored antiporter substrates and neurotoxic mechanisms, aiming to develop *in vitro* models for neurotoxicity predictions[95, 97, 98], the link between CNS drug exposure and drug-induced neurotoxicity still requires further investigation. To better understand this connection, advanced PK/PD investigations focusing on brain regions of interest (ROI) and antiporter substrates linked to neurotoxicity are essential.

Assessment of the rate and extent of CNS delivery

When a rapid therapeutic effect in the CNS is required, the rate of drug delivery to the CNS becomes a key consideration. For chronic treatments, the focus usually shifts towards the extent of drug delivery to the CNS. Therefore, both the rate and extent PK parameters are used to evaluate CNS drug delivery[99]. However, while these properties are interrelated, it is important to recognize that these are distinct properties and cannot be directly compared[6, 99]. Understanding both aspects may be crucial for optimizing drug development strategies for CNS disorders.

The CNS drug disposition of small molecular drugs is explained according to the free drug theory, i.e., it is only the unbound (free) drug that can diffuse across membranes and interact with pharmacological targets such as receptors, ion channels, transporters, and enzymes[100, 101]. Accordingly, the unbound drug concentration ratio across a CNS barrier determines the extent and net direction of drug transport, and it is the unbound drug at the site of action that may exert the pharmacological effect.

The extent of drug delivery to the brain is often described using partition coefficients[102]. The unbound partition coefficient ($K_{p,uu}$) is based on unbound drug concentrations in CNS compartments, such as brain ISF or CSF, to those in blood. For instance, $K_{p,uu,brain}$ is the ratio of the unbound drug in brain ISF to that in blood, which is calculated based on either steady-state concentrations or the area under the concentration-time curves (AUC):

$$K_{p,uu} = \frac{C_{u,CNS,ss}}{C_{u,blood,ss}} = \frac{AUC_{u,CNS}}{AUC_{u,blood}} \quad (1)$$

The net transport direction across brain barriers can be concluded from $K_{p,uu}$ values[103]. A $K_{p,uu}$ value of unity indicates passive transport or a balance between drug influx and efflux across the barrier. Values below unity suggest dominant efflux or other drug elimination processes, while values above unity indicate dominant influx[63, 99, 102]. Today, $K_{p,uu,brain}$ has become accepted as the best measure of the extent of BBB transport both in academia and industry[104]. In contrast, $K_{p,brain}$ reflects drug partitioning based on total concentrations in brain and plasma, which consequently also accounts for drug binding to brain tissue and plasma proteins[99].

In vitro, the rate of drug transport across brain endothelial cells (BECs) may be determined by flux or permeability (Eq. 2), and the extent by efflux ratio (ER, Eq. 3). The flux of drug transport is calculated as the accumulated drug amount transported across BECs divided by the surface area of the well where cells are seeded, and the incubation time. The apparent permeability (P) of the drug is obtained by dividing the flux by the difference in concentration (ΔC) between the apical and basolateral compartments:

$$P\ (\mathrm{cm} \times min^{-1}) = {Flux\ (\mathrm{nmol} \times cm^{-2} \times min^{-1})}\Big/{\Delta C\ (nmol \times cm^{-3})} \quad (2)$$

The ER is the ratio of drug permeability across the BEC layer from the basolateral to the apical side (B→A), to that from the apical to basolateral side (A→B):

$$ER = {P_{B\to A}}\Big/{P_{A\to B}} \quad (3)$$

These parameters are often used as predictions of drug CNS delivery in screening programs.

Assessment of intra-brain drug distribution

After a drug is transported across the BBB, it may further distribute within the brain, which is essential for the therapeutic effect of CNS drugs with intracellular targets. Intra-brain distribution involves the partitioning of drugs into cells and subcellular compartments, as well as their binding to brain tissue components, including proteins and membranes. To determine the extent of intra-brain distribution, the unbound drug concentration is related to the total drug concentration in the brain[6, 105]. This is assessed using the unbound volume of distribution within the brain ($V_{u,brain}$, mL×g brain^{-1}), which can be obtained during steady-state *in vivo* using total drug concentrations in the brain and unbound drug concentrations in brain ISF, typically through microdialysis[106, 107], or *in vitro* by the brain slice assay[108, 109]. $V_{u,brain}$ values provide insight into drug distribution, with values of 0.2 mL×g brain^{-1} suggesting that the drug distribution is limited to ISF, and values above 1.0 mL×g brain^{-1} suggesting tissue binding or active uptake into cells or distribution to subcellular organelles. The higher the $V_{u,brain}$ value, the more extensive brain tissue binding or distribution[6]. The fraction of unbound drug in the brain ($f_{u,brain}$) describes intra-brain distribution governed by the extent of brain tissue binding, typically assessed by equilibrium dialysis[110, 111].

Methods to study CNS drug disposition *in vivo* and *in vitro*

Both *in vivo* and *in vitro* methods are used to study CNS drug distribution (Figure 3). *In vivo* studies, typically conducted in rodents, offer valuable insights into how drugs behave in a complex biological system. In contrast, *in vitro* studies provide controlled environments that allow for investigations of

specific mechanisms. By combining *in vivo* and *in vitro* findings, a comprehensive understanding of how drugs reach and distribute within the brain can be achieved, which is critical for the development of safe and effective CNS therapies.

The BBB, consisting of multiple cell types *in vivo*, is modeled by endothelial cells *in vitro*. Plasma (*in vivo*), is mimicked by buffer *in vitro*, and interacts with the apical side of the endothelial cells. Brain ISF (*in vivo*) is also mimicked by buffer *in vitro*, and interacts with the basolateral side of the endothelial cells, as well as parenchymal cell membranes. Methods to investigate drug uptake into and/or transport across brain endothelial cells are *in vivo* microdialysis, the Combinatory Mapping Approach (CMA), or *in vitro* BBB cell models. The uptake into endothelial cells can be quantified using the unbound intracellular-to-extracellular concentration ratio ($K_{p,uu,cell}$). The extent of transport across endothelial cells can be determined by $K_{p,uu,brain}$ (Eq. 1, Eq. 4) or estimated by the *in vitro* ER (Eq. 3). The extent of drug accumulation in brain parenchymal cells can be investigated by $V_{u,brain}$ obtained by the brain slice method (Eq. 5). The extent of binding to components in any compartment, including plasma, cells (lysate) and brain tissue (homogenate), can be assessed by the fraction of unbound drug (f_u) obtained by equilibrium dialysis (Eq. 6). The parenchymal $K_{p,uu,cell}$ can be measured by combining data from the brain slice method and equilibrium dialysis, or predicted using the pH partitioning model[75].

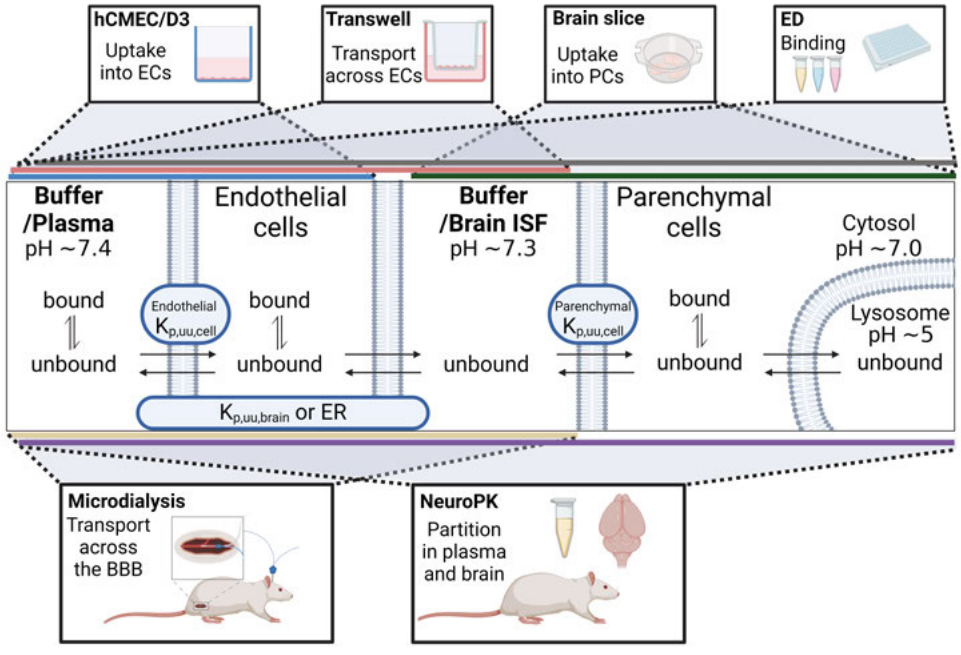

Figure 3. Schematic representation of plasma and brain compartments, and *in vitro* and *in vivo* methods used to study drug disposition. The colored bars along the compartments indicate the compartments that each method could characterize. *In vitro* methods: hCMEC/D3 (blue bar), Transwell (red bar), brain slice (green bar), and equilibrium dialysis (ED, gray bar). *In vivo* methods: microdialysis (yellow bar) and neuropharmacokinetic studies (neuroPK, purple bar). Within these compartments, the drug may be bound or unbound, where the unbound drug is available for transport across membranes by passive or active transport in both directions (indicated by arrows). As organic cation passive transport adheres to pH partitioning principles, pH values for each compartment are provided where known. EC, endothelial cell. PC, parenchymal cell. $K_{p,uu,cell}$, unbound endothelial cell-to-buffer concentration ratio. $K_{p,uu,brain}$, unbound brain ISF-to-plasma concentration ratio. ER, efflux ratio. BBB, blood-brain barrier.

Microdialysis

The optimal way to assess CNS drug delivery *in vivo* is to measure the unbound drug concentrations in CNS and blood. The only method for sampling unbound drug concentrations *in vivo* is microdialysis[112]. The technique is a gold standard method for the investigation of neuroPK and provides an opportunity to measure the extent of BBB and BCSFB transport using $K_{p,uu,brain}$ and $K_{p,uu,CSF}$[112]. Microdialysis involves probe placements in the site of interest and allows for dynamic assessment of unbound drug exposure with high spatiotemporal resolution in CNS and blood, and can be used to assess both the rate and extent of BBB and BCSFB transport *in vivo*. Microdialysis can be used in

humans, but due to its invasive nature, it is typically reserved for patients with conditions like traumatic brain injury[113]. The active uptake of oxycodone via the H^+/OC antiporter across the BBB was first identified in a study using microdialysis in rats, demonstrating a threefold higher concentration of unbound oxycodone in the brain compared to the blood[63].

CSF sampling

In humans, CSF is typically collected from the lumbar region of the spine[114]. Yet, due to its invasive nature, CSF sampling is not a routine method. CSF is often considered similar in composition to ISF[80, 114-116], and as CSF is more available for sampling than brain ISF, CSF is widely used as a surrogate for ISF to estimate brain drug concentrations in humans. However, the validity of using CSF as a surrogate for brain ISF has been questioned, particularly for drugs that are substrates of transporters[31, 114, 117-120]. Drug transport across the BBB and BSCFB may differ due to, for example, variations in the expression level of transporters[32], potentially leading to differences in fluid composition. Moreover, the extent to which molecules exchange between ISF and CSF is complex as it depends on both molecule- and CNS-related factors[15]. There is evidence suggesting that CSF concentrations often overestimate ISF concentrations of drugs that are efflux transporter substrates, whereas the opposite trend has been suggested for drugs with active uptake at the BBB[121]. $K_{p,uu,CSF}$ has been shown to be within threefold of $K_{p,uu,brainISF}$[121], which are sometimes considered "good enough" in drug development. A review of clinical reports and animal studies of the plasma-CSF-brain partitioning of 104 drugs with different physicochemical and PK characteristics, also found that ISF concentrations were generally lower than CSF concentrations[80]. However, the correlation between CSF and ISF for active uptake drugs, particularly for substrates of the H^+/OC antiporter system, needs further investigation.

The CMA

The CMA integrates *in vivo, in vitro,* and *in silico* neuroPK parameters[105]. This method serves as a screening toolbox to evaluate the extent of drug delivery across the BBB and parenchymal cell barriers, while also predicting intra- and subcellular drug distribution. It provides valuable insights for the evaluation and selection of CNS drug candidates in early drug discovery[79, 105, 122].

To obtain an overall picture of BBB transport and intra-brain distribution, *in vivo* measurements of the total partition coefficient, $K_{p,brain}$, are combined with *in vitro* $V_{u,brain}$ from brain slice studies[108, 109] and $f_{u,plasma}$ and $f_{u,brain}$ obtained by equilibrium dialysis[110, 111]. Further, the extent of intra- and subcellular drug distribution in the parenchymal cells, as determined by $K_{p,uu,cell}$, can be obtained by multiplying $V_{u,brain}$ with $f_{u,brain}$, or predicted using the pH partitioning model[75].

The CMA has been adapted for use in specific brain ROIs to evaluate regional differences in drug transport and distribution[13]. While CMA-ROI is effective for studying drug distribution across larger brain regions, its spatial resolution for smaller areas is limited. This limitation has been addressed by the development of a novel method using quantitative mass spectrometry imaging for unbound drugs (qMSI-uD), which allows for more precise quantification and visualization of regional differences in the extent of BBB transport[123].

In vitro BBB cell models

In vitro BBB cell models hold great potential for predictions of drug transport across the BBB[124], particularly valuable in CNS drug development due to their screening capabilities. Cell models derived from different species, such as humans, rats, and pigs, may possibly also provide insights into cross-species translation of drug transport, which is of great importance for bridging preclinical and clinical studies. However, for these models to be useful, they must reliably reflect *in vivo* conditions.

The human immortalized endothelial cell line, hCMEC/D3, provides a stable platform for studying uptake mechanisms[125, 126], and has been well-characterized for its brain endothelial phenotype. It has been suggested that the antiporter system functions in hCMEC/D3 cells[65, 69, 73, 127]. However, due to limitations in barrier integrity[124, 128], this model is more suitable for cellular uptake studies rather than transport studies, such as Transwell models. In contrast, primary BECs have been documented to maintain barrier properties including the expression of influx and efflux transporters and tight junctions, leading to restrictive drug permeability and high transendothelial electrical resistance (TEER)[129, 130]. As a result, primary BEC models are more suitable for Transwell studies, predicting both cellular drug uptake and release, enabling broader applications. The H^+/OC antiporter function is less studied in primary BEC models, yet there are studies in primary bovine[61, 131] and rat[53, 54] BECs.

A major challenge in using cell models is the uncertainty in how well their readouts correlate with *in vivo* data. For instance, the accuracy of Transwell BBB models replicating the *in vivo* BBB has recently been discussed based on differences such as the static (*in vitro*) versus dynamic condition (*in vivo*), the thick polystyrene semipermeable filter (*in vitro*) versus the basement membrane (*in vivo*), as well as the phenotype and function of cells[132]. Hence, there is a need for further investigations of the performance of these models. Additionally, *in vitro*-derived ER, commonly used in drug selection[124], often shows discrepancies with unbound brain-to-blood ratios *in vivo*[133], suggesting that these models may need refinement to better mimic *in vivo* conditions. Using clinically relevant drug concentrations *in vitro* may be one step towards this goal.

Moreover, when comparing data, it is essential to ensure that readouts from different models reflect the same parameter. For example, as highlighted by

Hammarlund-Udenaes et al., a high transport extent may not correspond to a high transport rate, and can therefore, not be directly compared[99]. Also, the nomenclature of parameters can vary between methods, even when describing the same processes, for example, $V_{u,brain}$ and $K_{p,uu,cell}$. Harmonizing readouts and nomenclature across models is, therefore, essential to avoid misinterpretations.

Inflammation as a model for pathology

As inflammation is common in several CNS disease conditions[8], it is crucial to investigate its impact on drug PK and CNS disposition. For this reason, inflammation models are often used in preclinical studies[134]. Various approaches are used to induce inflammation *in vivo*, including systemic- or CNS injections of cytokines or bacterial toxins [134]. The bacterial toxin, lipopolysaccharide (LPS), has been well documented to activate the immune response, triggering the expression of a wide range of inflammatory mediators[134, 135]. This immune response has also been clinically associated with harmful consequences[136-138]. Due to its properties, LPS has been described as one of the most effective stimulators of the immune system and one of the most potent pro-inflammatory agents that release pro-inflammatory cytokines and acute phase proteins[139, 140]. LPS is therefore commonly used to induce inflammation in various species[50, 51, 134, 139, 141-143]. Nazem et al. even suggest that LPS challenge is the standard model for studying neuroinflammation[144]. The origin of LPS and dosing regimen vary widely in the literature[134].

However, the impact of inflammation on the rate and extent of antiporter substrate transport is not well understood with studies reporting conflicting results. For instance, the extent of diphenhydramine brain uptake has been reported both to increase and decrease under inflammation conditions[53, 54]. Meanwhile, the extent of oxycodone brain delivery has been reported as unchanged in models mimicking Alzheimer's (aged AβPP-transgenic mice) and Parkinson's (α-synuclein transgenic mice) diseases[145]. Similarly, in a non-inflammatory pericyte-deficient mouse model, no differences in either the extent or rate of drug transport across the BBB were observed compared to healthy mice[146, 147]. Together, these findings underscore the need for further research to clarify the conflicting conclusions regarding the influence of inflammatory conditions on antiporter substrate's brain uptake.

In vitro, it is more difficult to obtain the full immune response observed *in vivo*. Yet, simpler approaches are often used to study the effect of immune response components, such as individual or combinations of cytokines. For instance, interleukin (IL) 6, which is a key cytokine released during inflammation *in vivo* [148-150], was reported to disrupt the barrier integrity of primary rat BECs[151]. Regarding the H^+/OC antiporter function, it is not fully understood if individual immune response components can impact its expression level and function. So far, tumor necrosis factor-alpha (TNF-α) and IL-1β

have been reported without effect on the cell drug exposure of diphenhydramine in primary rat BEC[54].

Aims of the thesis

The overall aim of this thesis was to investigate CNS drug distribution with focus on the role of the H^+/OC antiporter system. By examining species and sex differences, disease conditions, *in vitro–in vivo* correlations, and regional CNS distribution, the goal was to enhance the translation of preclinical findings to clinical applications and improve the development of effective and safe CNS-targeted therapies.

More specifically the aims were to:

- Investigate the role of the antiporter system across various CNS barriers (Papers I, III, V)
- Investigate the impact of LPS-induced inflammation on the systemic and CNS PK of oxycodone as an antiporter model substrate (Papers II-III)
- Explore variations in the systemic and CNS PK of oxycodone across sexes and species (Papers I–III)
- Correlate PK findings between *in vitro* and *in vivo* studies to validate the utility of *in vitro* BBB models for investigation of active uptake (Paper IV)
- Assess the regional CNS drug disposition for selected antiporter substrates, to explore their neuroPK in relation to neurotoxicity (Paper V)

Material and Methods

Selection of drugs

Previously reported substrates of the H^+/OC antiporter system were selected for studies included in this thesis[62]. Oxycodone was used as the main model substrate in all papers as it has been confirmed as a substrate in *in vitro* BBB models[64] and with a net uptake at the BBB *in vivo*[63]. Another important aspect for the selection of oxycodone was its compatibility with microdialysis, as this technique is not suitable for many compounds. In Paper V, memantine, bupropion, diphenhydramine, oxycodone, pyrilamine, and tramadol were selected due to their association with neurotoxicity, as identified also through pharmacovigilance data. Diphenhydramine, bupropion and tramadol[95], pyrilamine[152, 153], and oxycodone[154] have been associated with DIS, while memantine has been associated with MCAEs[94]. In all studies, the drug dosing regimens were chosen based on therapeutically relevant plasma and brain concentrations.

Animals

Female and male Sprague-Dawley rats (Taconic, Lille Skensved, Denmark) with body weights of 270–330 g were used for studies in Papers I–II and IV–V. The rats were group-housed by sex under a 12-hour light-dark cycle at 20–21°C and 45–65% humidity with free access to food and water. Before experiments, the rats were acclimatized for one week. The studies were approved by the Animal Ethics Committee of Uppsala, Sweden (Ethical Approval Dnr. 5.8.18-12230/2019).

Female and male Swedish landrace pigs with body weights of 29.8±1.6 kg were used for experiments in Paper III. The pigs were transported from the breeder to Uppsala University on the day of the experiment. The study was approved by the Animal Ethics Committee of Uppsala, Sweden (Ethical approval Dnr. 5.8.18-12768/2021).

Isolation of primary mouse and rat BECs (Paper IV) was performed at the University of Copenhagen, while isolation of primary pig BECs was performed at Aarhus University (Denmark). Female and male C57Bl/6 mice and Sprague-Dawley rats (Envigo, Horst, Netherlands) were group-housed by species and sex similarly as described above. The mice and rats were acclimatized

for two weeks before brain isolation. The pig brains were collected from female and male pigs at a slaughterhouse (Horsens, Denmark), and transported to Aarhus on ice.

All animal studies in this thesis were conducted in compliance with regulations of the Swedish Animal Welfare Agency, guidelines from the Swedish National Board for Laboratory Animals or the Danish Animal Welfare Act, and the European Communities Council Directive of 22 September 2010 (2010/63/EU). The studies were performed with efforts made to minimize the number of animals and reduce their suffering while maintaining sufficient statistical power of the studies, and the minimal sample size per group was estimated using pilot studies and power and sample size calculations[155]. None of the animal studies were randomized or blinded.

Experimental procedures

In this thesis, a variety of experimental methods were employed, including microdialysis, *in vivo* PK studies, the brain slice assay, equilibrium dialysis, and *in vitro* BBB cell culture studies (Figure 3).

To assess the systemic PK and CNS disposition of oxycodone in health and disease, *in vivo* microdialysis was performed in rats (Papers I–II) and pigs (Paper III) of both sexes. In Paper I, the rats were healthy, whereas in Paper II, the rats were challenged with LPS to induce inflammation. Pigs in Paper III underwent microdialysis during a healthy period followed by an LPS-induced inflammation period. These studies required extensive surgical preparations.

To investigate the intra-brain drug distribution in rats and pigs, brain slice experiments (Papers I, IV–V) and equilibrium dialysis were performed (Papers I, III–V). To enable these experiments, plasma from rats was collected under inhalation anesthesia, and brains were isolated following decapitation. In pigs, plasma was collected under intravenous anesthesia and brains were isolated post-mortem.

To assess the regional CNS distribution of drugs in Paper V, the CMA approach was employed. Rats underwent *in vivo* PK experiments which involved less extensive surgical preparations compared to microdialysis. Thereafter, data from the *in vivo* PK study were combined with data from brain slice and equilibrium dialysis experiments.

To evaluate the *in vitro* uptake and transport of oxycodone and pyrilamine, *in vitro* BBB cell models from rat and human origins were used (Paper IV). Additionally, pilot studies using *in vitro* BBB cell models from mouse and pig origins were conducted to explore potential differences in the uptake between these models (unpublished). Primary mouse, rat, and pig BECs were used for drug transport studies in Transwell systems, while the human hCMEC/D3 cell line was used for drug uptake studies, with cells cultured on the bottom of the wells. Pre-treatment with IL-6 was used in hCMEC/D3 cells to investigate the

cytokine's impact on cellular uptake. The performance of the various models and their correlation with *in vivo* data were evaluated.

Animal surgeries for *in vivo* experiments

In rats (Papers I–II and V), anesthesia was induced and maintained by inhalation of isoflurane, supplemented with oxygen. The rats were kept on a heating pad with continuous body temperature monitoring. Preparations of rats for the *in vivo* studies included catheterization of the vein and artery (Papers I–II and V). For the microdialysis studies, the catheterization was followed by placement of microdialysis probes (Papers I–II). Postoperative, all rats were administered isotonic saline solution subcutaneously, to maintain a healthy hydration, supplemented with buprenorphine for pain relief. Thereafter, the rats were placed in a CMA/120 system for freely moving animals and allowed to recover for 24–28 hours before the experiment.

The pigs in Paper III were monitored as intensive care patients by trained personnel throughout the experiment, and a more extensive surgical preparation was required. Upon arrival, anesthesia was induced by intramuscular injection of tiletamine, zolazepam, and xylazine. Later, anesthesia was maintained by an intravenous infusion of a glucose solution supplemented with ketamine, fentanyl, and midazolam. To support the body temperature, the pigs were kept on a heating pad. The preparation of the pigs included set up of health monitoring equipment, catheterizations, and placement of microdialysis probes.

Preparations of the pigs

To ensure pain relief prior to surgery, fentanyl was administered intravenously. To prevent shivering, muscle relaxation was achieved with intravenous rocuronium. Throughout the surgery and experiment, monitoring of the pig was performed using an IntelliVue MP50 patient monitor to track body temperature, blood pressure, oxygen saturation, and electrocardiography. If necessary, noradrenaline was infused to maintain a mean arterial pressure above 60 mmHg. Tracheotomy was performed, and mechanical ventilation was provided with a Maquet Servo-I ventilator. Normoventilation was maintained by adjusting the tidal volume, and oxygen saturation was monitored using a pulse oximeter probe placed on the tail, with an oxygenation target of 10-30 kPa achieved by adjusting the fraction of inspired oxygen. Positive end-expiratory pressure was increased in cases of repeated hypoxemia. Blood gas analysis was used to monitor acid-base balance, electrolytes, hematocrit, hemoglobin, and glucose levels. A healthy hydration was maintained with a continuous intravenous administration of an electrolyte solution. For practical reasons, a urinary catheter was surgically inserted into the urinary bladder to collect urine. A small cervical artery was catheterized to sample blood and monitor blood pressure, while the external jugular vein was catheterized for infusions and additional blood pressure monitoring.

Placement of microdialysis probes and epidural catheters in rats and pigs

Following catheterization and other preparations, microdialysis probes were inserted in blood and CNS compartments for microdialysis studies in rats and pigs to obtain unbound concentrations at the sites of interest (Papers I–III). Additionally, in pigs, an epidural catheter was placed in the lumbar region of the spine for CSF sampling.

In rats undergoing microdialysis probe placement (Papers I–II), the anesthesia was supplemented with nitrous oxide in addition to oxygen, to ensure pain relief. A 10 mm CMA 20 Elite probe was inserted into the right jugular vein through a guide cannula and fixed to the pectoral muscles. For CNS probe placement, the rats were placed in a stereotaxic instrument to position the head. Coordinates obtained from the Rat Brain atlas[156] were used to accurately place CMA 12 Elite probes in two of the following sites: striatum (3 mm probe membrane), lateral ventricle, and *cisterna magna* (1 mm probe membrane). To place each probe, a probe guide was first anchored to the skull at the specified coordinates, followed by insertion of the probe into the guide.

In pigs (Paper III), custom-made microdialysis probes were placed in the femoral vein, frontal brain cortex, and lateral ventricle (CMA 20 Elite probes, 10 mm membrane). The blood probes were placed in the vein through an intravenous catheter. The CNS probes were placed through burr holes in the skull and fixed using a bolt and intravenous catheter, and bone wax if needed. To support the correct placement of the lateral ventricle probe, ultrasound was used. An epidural catheter was placed intrathecally in the lumbar region of the spine to collect lumbar CSF. Post-surgery, pigs were allowed to recover for 90 minutes before initiation of drug infusion.

Microdialysis to evaluate the CNS disposition of oxycodone in rats and pigs

Following post-surgical recovery, the rats (Papers I–II) and pigs (Paper III) underwent oxycodone microdialysis experiments. The experimental designs for the microdialysis studies in rats are illustrated in Figure 4, while the design for the pig study is illustrated in Figure 5. Although the study designs varied slightly between studies, they all included a stabilization period followed by drug administration.

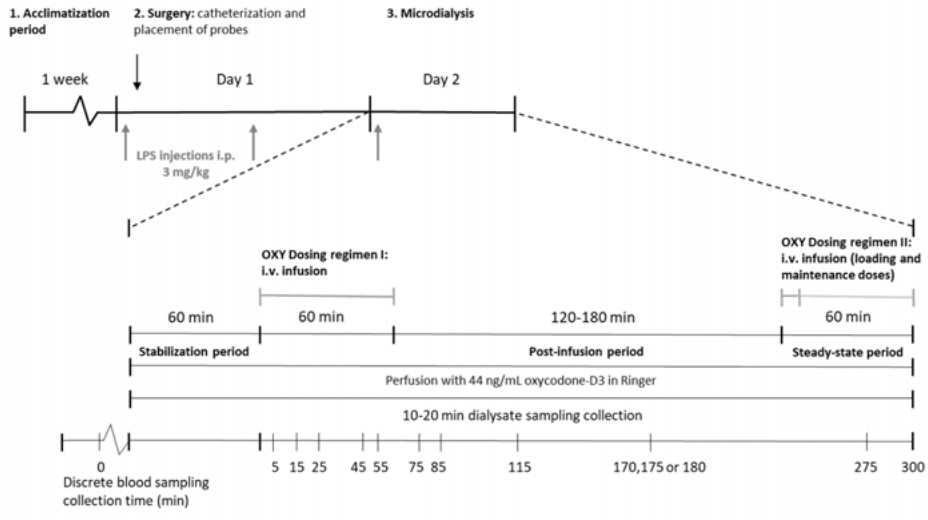

Figure 4. Schematic overview of the experimental design of the microdialysis studies in healthy (Paper I) and lipopolysaccharide (LPS)-treated rats (Paper II). In healthy rats, surgery was performed 24 hours before the microdialysis experiment. In LPS-treated rats, the first LPS dose was administered 28 hours before oxycodone administration, followed by surgery. The LPS dosing regimen consisted of three intraperitoneal injections of 3 mg/kg, administered at times 0, 6, and 24 hours. In both studies, the experiment was initiated by a 60-minute stabilization period, followed by two oxycodone dosing regimens separated by a washout period. Oxycodone Dosing regimen I consisted of a 60-minute intravenous infusion (0.3 mg/kg/h). Oxycodone Dosing regimen II included a two-minute intravenous infusion (0.24 mg/kg), followed by a 60-minute maintenance infusion (0.54 mg/kg/h). Throughout the experiments, dialysate, plasma, and blood cell samples were collected, and the brain was isolated terminally.

The microdialysis experiments (Figure 4 and Figure 5) began with a stabilization period, during which the microdialysis probes were perfused with CNS Ringer's solution containing the calibrator oxycodone-D3, at a perfusion rate of 1 µL/min. This perfusion was maintained throughout the experiments. Thereafter, the animals received oxycodone via intravenous infusions.

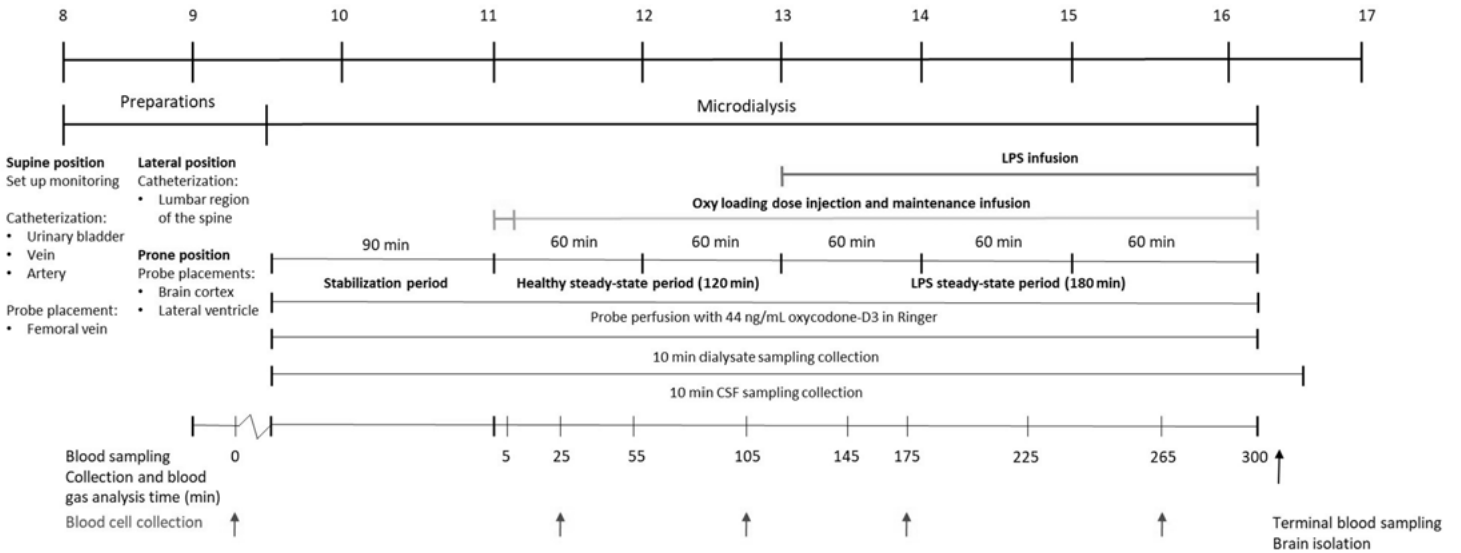

Figure 5. Schematic overview of the experimental design of the microdialysis study in pigs (Paper III). After the preparation of the pig, recovery was allowed for 90 minutes while a stabilization period was performed. Thereafter, oxycodone was administered as an intravenous loading dose (0.16 mg/kg) over two minutes, followed by a maintenance infusion (0.05 mg/kg/h) over five hours. A concomitant LPS infusion of 4 µg/kg/h was initiated 120–150 minutes after the start of the oxycodone infusion. Throughout the experiment, dialysate, lumbar cerebrospinal fluid (CSF), plasma, and blood cell samples were collected, and the brain was isolated terminally.

Microdialysis probe recovery determination

To estimate the recovery of oxycodone across the microdialysis probe membranes, *in vivo* retrodialysis by the calibrator oxycodone-D3 was used (Paper I–III)[157]. Oxycodone-D3 is an optimal calibrator as it is a deuterated analog of oxycodone with structural similarity, hence, their probe recoveries were assumed to be equivalent. For all rat and pig experiments (Papers I–III), each specific probe recovery as well as the mean recovery for each specific probe membrane length and location were determined, as recovery is influenced by factors such as probe length and properties of the surrounding tissue or fluid[112]. The recovery for probes used in the different CNS compartments and blood were determined for rats and pigs, respectively.

Unbound concentrations in blood and CNS compartments were obtained by dividing the dialysate concentrations by the probe recovery, compensating for the incomplete recovery of oxycodone across the probe membranes. In rats (Papers I–II), unbound concentrations were obtained by using the mean recovery of probes of the same membrane length in the CNS, i.e., striatum (3 mm), and lateral ventricle and *cisterna magna* (1 mm), respectively. Unbound blood concentrations were determined using each rat's individual blood probe recovery. If the recovery was unusually low or unrealistic, the location-specific mean recovery from the other rats was used. In pigs (Paper III), the probe recoveries generally fluctuated more over time. To account for these changes, a moving average recovery was applied[157]. For each dialysate sample, the mean recovery was calculated using the calibrator recovery from three consecutive dialysate samples centralized around the specific sample interval.

Inflammation models

LPS-induced inflammation in rats and pigs

In both rats (Paper II) and pigs (Paper III), LPS was used to induce inflammation and assess oxycodone PK and CNS delivery under a pathological condition. The key differences between the inflammation models are the i) bacteria strain from which LPS was derived, ii) LPS route of administration, and iii) incubation time allowed for the LPS to induce inflammatory responses.

Rats were administered LPS from *Salmonella typhimurium* in three intraperitoneal doses (3 mg/kg) before surgery (time 0), and at 6 and 24 hours later, resulting in a total LPS dose of 9 mg/kg. The choice of bacterial strain from which the LPS was derived and dosing regimen was based on previously established protocols in mice[50, 142, 143]. The oxycodone infusion was initiated 28 hours after the first LPS dose to allow for post-surgery recovery and LPS incubation time. Inflammation was confirmed through proteomic analysis of plasma and brain samples using the Target 96 Mouse Exploratory panel (Olink Proteomics AB) quantifying inflammation biomarkers. These samples were collected from both LPS-treated and healthy rats, with sample preparations performed according to Olink's instructions.

In pigs, the LPS-induced inflammation was initiated after a control period of 120–150 minutes. The inflammation period of 150–180 minutes was adapted from previous pig studies using LPS from *Escherichia coli* as an intravenous infusion (4 μg/kg/h). This regimen was previously documented to induce physiological changes, elevated cytokine levels (TNF-α and IL-6), and septic-mimicking conditions in pigs[149, 158-160]. To evaluate the extent of organ failure and severity of the LPS-induced inflammation, the Sequential Organ Failure Assessment (SOFA) adapted for pigs was used[161].

Evaluation of BBB integrity in healthy and LPS-challenged rats

In Paper II, the BBB integrity was evaluated in healthy and LPS-treated rats by assessing the extent of BBB transport of a fluorescent 4 kDa tetramethylrhodamine B isothiocyanate (TRITC) dextran as described previously[162, 163]. In these rats, the surgery involved vein and artery catheterization and placement of a microdialysis probe guide in the striatum, as described above. At 24–28 hours after the surgery, the BBB integrity experiment was performed. Rats received an intravenous infusion of the TRITC dextran of 400 mg/kg over five minutes. Blood samples were collected both before and five minutes after the start of the infusion. At the end of the infusion, terminal blood was collected via heart puncture, and the rats were transcardially perfused with isotonic saline at a rate of 10 mL/min for two minutes to eliminate blood that would contaminate the brain for assessment of the total dextran brain-to-serum concentration ratio, $K_{p,brain}$.

The sampled serum was diluted in MilliQ water and stored at 6°C until bioanalysis. The brain was isolated and dissected to evaluate if the BBB integrity varied between the whole brain and striatum at the site of probe guide placement and striatum on the contralateral side. Brain tissue was homogenized in MilliQ water, centrifuged and the supernatants were collected for analysis.

The fluorescence intensity of the TRITC dextran was measured using a Tecan Spark® Multimode Microplate Reader, with excitation at 550 nm and emission at 571 nm. $K_{p,brain}$ was calculated using the terminal blood and brain samples.

CMA-ROI to evaluate regional CNS exposure of antiporter substrates

In Paper V, regional CNS exposure of H^+/OC antiporter substrates with associations to neurotoxicity was investigated using the CMA-ROI applied to rat data. To evaluate the extent of transport to brain regions, spinal cord, and CSF as reflected by $K_{p,uu}$ and into parenchymal cells reflected by $K_{p,uu,cell}$, *in vivo* PK studies, brain slice, and equilibrium dialysis were performed. The extent of drug transport across the BBB in the brain ROIs and across the BSCB was

determined unbound ROI-to-plasma concentration ratio ($K_{p,uu,ROI}$) calculated as follows:

$$K_{p,uu,ROI} = \frac{K_{p,ROI}}{f_{u,plasma} \times V_{u,brain}} \quad (4)$$

Where $K_{p,ROI}$ is the total ROI-to-plasma drug concentration ratio, $f_{u,plasma}$ the fraction of unbound drug in plasma, and $V_{u,brain}$ the unbound volume of drug distribution in the brain. The extent of drug transport across the BCSFB was assessed by $K_{p,uu,CSF}$, calculated using Eq. 1, assuming that the drug is fully unbound in CSF, while $C_{u,plasma,ss}$ was derived from $C_{tot,plasma,ss}$ and $f_{u,plasma}$. The extent of parenchymal cell drug uptake ($K_{p,uu,cell}$) was calculated by multiplying $V_{u,brain}$ with $f_{u,brain}$. As $K_{p,uu}$ and $K_{p,uu,cell}$ estimates are derived from multiple parameters with their respective uncertainties, the standard deviations were estimated using the propagation of error method[164]. Regional data were compared with whole brain data to examine the heterogeneity of BBB, BSCB, and BCSFB transport, as well as intra-brain distribution.

In vivo PK study in rats

To obtain the total CNS region-to-plasma concentration ratios, including brain regions and spinal cord ($K_{p,ROI}$) as well as CSF ($K_{p,CSF}$), *in vivo* PK studies were conducted in healthy rats. To minimize animal use, single time-point steady-state assessments were performed. After catheterization of the vein and artery followed by a 24-hour recovery period, each rat was administered one of the following drugs: memantine, bupropion, diphenhydramine, oxycodone, pyrilamine, and tramadol. The drug was administered intravenously as a loading dose followed by a four-hour maintenance infusion to achieve steady-state. Blood samples were collected from the artery catheter throughout the experiment at specified time points. At 4 hours, while the infusion was still ongoing, the rats were anesthetized and placed in a stereotaxic apparatus for CSF collection from the *cisterna magna*. Thereafter, blood was sampled by cardiac puncture, and the brain and spinal cord were collected. One hemisphere was collected as a whole brain, and the other was dissected into ROIs, including the cerebellum, frontal cortex, parietal cortex, striatum, and hippocampus. All samples were weighed and stored at –80°C pending analysis. Before bioanalysis, brain regions and spinal cord were homogenized in four volumes of phosphate-buffered saline (PBS).

Brain slice assay to evaluate intra-brain distribution

In Papers I and IV–V, the brain slice assay was used to determine $V_{u,brain}$. This method is designed to assess the relationship between the total drug concentration in the brain and the unbound drug concentration in artificial extracel-

lular fluid (aECF) under *in vitro* conditions, resembling brain ISF concentrations *in vivo*. Immediately after isolation, the brains were transferred to ice-cold, pre-oxygenated, blank aECF. For all studies, six coronal slices of 300 µm were prepared from drug-naïve rat brains using a Leica VT1200 microtome slicer. The slices were incubated in pre-oxygenated aECF containing the drug of interest. In Paper I, the aECF contained oxycodone at concentrations of 30 and 300 ng/mL (≈95 and 950 nM) to mimic the *in vivo* unbound brain ISF concentration. In Paper IV, oxycodone incubation concentrations of 100–5000 nM were used to assess concentration-dependent oxycodone intra-brain distribution. In Paper V, the brain slice method was extended to assess the intra-brain distribution of various drugs (pyrilamine, diphenhydramine, bupropion, tramadol, oxycodone, and memantine) at 100–200 nM, as well as the impact of a 30-minutes pre-incubation with the intracellular pH modulators monensin (50 nM) and bafilomycin A1 (10 nM).

The drug incubation was carried out at 37°C for 5 hours with constant oxygenation and orbital shaking at 45 rpm in a MaxQ4450 incubator. After incubation in Paper I, each brain slice was cut into two halves, with one half used as whole brain tissue and the other used to micro-dissect the striatum. No micro-dissection of brain slices was performed after incubations in Papers IV–V. The brain tissues were dried, weighed, and homogenized in aECF. Before bioanalysis, the buffer and brain homogenate samples were matrixed matched, by adding blank buffer to the homogenate samples and blank homogenate to the buffer samples, followed by storage at –20 °C. Assuming equilibrium was reached, $V_{u,brain}$ was calculated based on the drug amount in the brain slices and the concentration in the buffer, with corrections for the volume of aECF surrounding the slices, using the following equation:

$$V_{u,brain} = \frac{A_{brain} - V_i \times C_{u,buffer}}{C_{u,buffer} \times (1 - V_i)} \quad (5)$$

Where A_{brain} is the drug amount in the brain tissue, V_i the volume of remaining aECF surrounding the brain slice (0.133 mL×g brain^{-1},[162]), and $C_{u,buffer}$ the unbound drug concentration in aECF.

Equilibrium dialysis to evaluate drug binding

In Papers I and III–V, the equilibrium dialysis method was utilized to evaluate the f_u in plasma, brain, and hCMEC/D3 cells[110, 111, 165], with slight variations across the projects based on the biological matrix, its origin, and the spiking-concentration of the drug. Before dialysis, plasma was undiluted, brain tissue was homogenized in PBS (1:9) and hCMEC/D3 cells were lysed in lysis buffer (0.1% Triton X100, 0.95:200 µL).

In Paper I, $f_{u,plasma}$ and $f_{u,brain}$ were determined in healthy rat samples. In Paper III, $f_{u,plasma}$ and $f_{u,brain}$ were determined using samples from healthy and

LPS-treated pigs. In Paper IV, $f_{u,cell}$ were assessed in hCMEC/D3 cells. In Paper V, $f_{u,plasma}$ was assessed using healthy rat samples, and the method was extended to evaluate the binding in various CNS ROIs, including $f_{u,ROI}$ in the frontal cortex, parietal cortex, cerebellum, striatum, hippocampus, and spinal cord.

The matrix (plasma, brain homogenate, or hCMEC/D3 lysate) was spiked with the drug of interest at *in vivo*-relevant concentrations. A Teflon 96-well plate with a semipermeable membrane (12–14 kDa) was used for dialysis, the biological matrix was dialyzed against an equal volume of PBS for 6 hours at 37°C with continuous orbital shaking at 200 rpm in the MaxQ4450 incubator. Biological matrix and buffer samples were collected after the 6-hour dialysis, matrix-matched, and stored at –20°C for bioanalysis. The f_u was calculated as the ratio of unbound drug concentration in the buffer to the total concentration in the corresponding biological matrix.

As the brain and cells are diluted before equilibrium dialysis, the dilution must be considered for the calculation of $f_{u,brain}$ and $f_{u,cell}$, according to the following equation:

$$f_u = \frac{\frac{1}{D}}{\left(\left(\frac{1}{f_{u,D}}\right)-1\right)+\frac{1}{D}} \quad (6)$$

Where D is the dilution factor, which was 10 for brain and 211.5 for hCMEC/D3, and $f_{u,D}$ is the ratio of unbound drug in the buffer-to-diluted tissue.

Evaluation of BBB cell model's potential for investigating active uptake

Culturing primary BECs

Primary BECs were isolated from mice, rats[166], and pigs[167] according to previously published protocols. Briefly, the brains were harvested, and meninges removed. The brain tissue was homogenized in Dulbecco's Modified Eagle's Medium (DMEM), followed by the performance of multiple filtering and centrifugation steps to isolate capillaries. The capillary fragments were digested enzymatically and further processed to obtain a suspension of BECs in DMEM. Mouse and rat BECs were cultured immediately after isolation while pig BECs were frozen and stored in a cryotank with liquid nitrogen before culturing. At the time of culturing, cells were first cultured on collagen and fibronectin-coated flasks and, thereafter, seeded on Transwell inserts. The cells were maintained under standard culture conditions (37°C, 5% CO_2), and after 4–10 days, the *in vitro* BBB models were ready for use, confirmed by measuring TEER. The drug transport studies across the BECs were performed

in differentiation media containing DMEM supplemented with components to promote cell health and maturation.

Drug uptake and transport studies in primary BECs

Drug transport studies were performed using primary BECs. The transport of oxycodone and ^{3}H-pyrilamine into and across the BECs was evaluated in both directions (apical to basolateral, A→B, and basolateral to apical, B→A). Oxycodone or ^{3}H-pyrilamine was added to the donor compartment, and samples were collected initially and terminally from the donor compartment, and the receiver compartment at 20-minute intervals during 120 minutes. After the experiment, TEER was measured, and cells were lysed for further analysis. Drug concentrations in the donor, receiver, and cells were quantified, and the rate and extent of drug transport into and across the cells were calculated. Flux and permeability were used as rate parameters. Flux was calculated at each sampling time point by dividing the accumulated drug amount transported across BECs into the receiver compartment at that time point with the product of the surface area of the well (0.336 cm^2) and incubation time. The apparent permeability was obtained by dividing the flux with the concentration gradient, which was assumed to be equal to the donor concentration due to sink conditions (Eq. 2).

The extent of drug uptake into BECs was calculated as the total cell-to-unbound buffer concentration ratio ($K_{p,u,cell}$). Thereafter, $K_{p,uu,cell}$ was obtained by multiplying $K_{p,u,cell}$ and $f_{u,cell}$ using the propagation of error method as described for parenchymal $K_{p,uu,cell}$. The extent of transport across BECs was calculated as ER (Eq. 3). The *in vitro* $K_{p,uu,brain}$ was obtained by inverting the ER.

Culturing immortalized brain endothelial hCMEC/D3 cells

hCMEC/D3 was cultured in an endothelial basal medium (EBM®-2) supplemented with growth factors and 5% fetal bovine serum. Cells were first cultured on collagen-coated flasks and, thereafter, seeded on 24-well plates and used for experiments after four days. The cells were maintained under standard culture conditions.

Drug uptake studies in healthy and interleukin-6-treated hCMEC/D3

Oxycodone uptake into hCMEC/D3 cells was evaluated under both healthy and IL-6 pre-treated conditions to assess the rate and extent of uptake and the impact of the cytokine. The studies were conducted by incubating hCMEC/D3 cells with oxycodone at concentrations of 10–5000 nM for incubation times of 2–60 minutes, to examine concentration- and time-dependent uptake. After incubation, the cells were washed, lysed, and stored at –80°C prior to bioanalysis. Flux was calculated as the accumulated drug amount in the cells divided by the product of the surface area of the well (1.9 cm^2) and incubation time. Partition coefficients, $K_{p,u,cell}$ and $K_{p,uu,cell}$, were calculated as described for primary BECs. Michaelis-Menten kinetic parameters were determined by fitting the data to the model using Graph Pad Prism (version 9.0.0 for Windows).

Bioanalysis of drugs

UPLC-MS/MS

In all studies (Papers I–V), reversed-phase liquid chromatography coupled with mass spectrometry was used to quantify the drugs of interest and their respective internal standards across various matrices, including plasma, blood cells, brain and spinal cord tissue homogenates, CSF, dialysate, BBB cell lysate and cell media. An Acquity Ultra-Performance Liquid Chromatography (UPLC) system coupled with a Xevo TQ-S Micro mass spectrometer (Waters Corporation) was used to quantify oxycodone, oxycodone-D3, pyrilamine, bupropion, diphenhydramine, and tramadol. Memantine was quantified using a Quatro Ultima™ PT triple quadrupole mass spectrometer (Micromass) coupled with an HPLC system equipped with LC-10ADvp pumps and a SIL-HT autosampler. Detection of all compounds was carried out using mass spectrometry multiple reaction monitoring mode, allowing for the monitoring of parent-to-product ion transitions for accurate quantification.

The analytical methods were developed by optimizing system parameters to achieve high resolution within a reasonable analysis time. Data analysis and quantification were performed using MassLynx and TargetLynx (Waters Corporation). Standard curves were adapted to match the expected sample concentrations and demonstrated good linearity ($R^2 > 0.99$), with all samples within the linear range. Quality control samples were included at a minimum of three concentration levels distributed across the standard curve range. Sample preparation typically involved protein precipitation, followed by centrifugation and supernatant dilution, with minor variations between projects.

Liquid scintillation counting

The quantification of ^{3}H-pyrilamine in cell lysate and cell media samples from the BEC transport studies in Paper IV was performed immediately after the experiment. Samples were mixed with 2 mL of Ultima Gold™ 241 scintillation cocktail (Perkin Elmer) and analyzed using a Tri-Carb 2910 TR Liquid Scintillation Analyzer (Perkin Elmer).

Statistical analysis

In all papers, statistical analyses were conducted using the GraphPad Prism software (version 9.0.0 for Windows). Statistical significance was set at $p < 0.05$, with data presented as mean values and standard deviations if nothing else is stated. A variety of statistical tests were applied to analyze the data, with specific methods tailored to each study design and objective. Normality tests were performed to ensure normal distribution of data, to enable parametric statistical methods. Generally, two-tailed t-tests (paired or unpaired) were

used to compare means between two groups, while one-way ANOVA followed by multiple comparison tests was employed for comparing multiple groups. Two-way ANOVA followed by appropriate post-hoc tests was used to compare groups across two factors. In cases with missing data points, mixed-effects models were applied to ensure robust analyses. To assess the relationship between variables, correlation coefficients, including Pearson correlation, were used.

Additionally, specific statistical methods were used depending on the study focus. In Paper II, proteomic data of inflammation biomarkers were analyzed using an ANOVA F-test with correction for multiple comparisons, followed by post-hoc analysis to identify significant changes in protein levels. Principal component analysis (PCA) was also used to visualize patterns in the data. In Paper IV, Michaelis-Menten modeling was performed to describe the kinetics of drug uptake *in vitro*. In Paper V, the Brown-Forsythe Test was used to compare the equality of variances between groups.

Results and Discussion

The studies presented in this thesis demonstrate an active uptake of antiporter substrates across various CNS barriers. The uptake was sex-independent with minimal variations across rats and pigs. Studies under LPS-induced inflammation revealed a reduced extent of substrate uptake, although a preserved net uptake. The consistent net uptake, with minimal brain region variability, is contributing to a high CNS exposure of antiporter substrates which may contribute to the previously documented association with drug-induced neurotoxicity. Uptake data of antiporter substrates in BEC models derived from human, mouse, rat, and pig sources suggest that these models hold the potential to characterize active drug uptake to the brain.

Active CNS barrier uptake of antiporter substrates in rats and pigs (Papers I, III, V)

Presence of active uptake of antiporter substrates at the BBB, BCSFB, and BSCB in rats and pigs

Studies described in Papers I, III, and V investigated the role of the H^+/OC antiporter system in transporting oxycodone and other substrates across the BBB, BCSFB, and BSCB. Microdialysis was used in Papers I and III focusing on oxycodone transport in rats and pigs, respectively, while the CMA-ROI method was used to expand the investigation to multiple antiporter substrates in Paper V.

Papers I and III provided novel *in vivo* evidence of active oxycodone uptake at both the BBB and BCSFB, indicating the likely presence of the antiporter system across rats and pigs (Figure 6). In rats, the net uptake was reflected by a $K_{p,uu,brain}$ of 4.44 and a $K_{p,uu,LV}$ of 3.41 (Figure 6A), and consistent with the previously reported $K_{p,uu,brain}$ of 3[63]. Further, the studies provide the first evidence of active oxycodone uptake across the BBB in pigs with a $K_{p,uu,brain}$ of 2.5 (Figure 6D), supporting the hypothesis of a preserved H^+/OC antiporter system in higher species, potentially also extending to humans. Despite considerable variability in pig lateral ventricle measurements, data also suggests active uptake at the pig BCSFB, with a mean $K_{p,uu,LV}$ of 2.4, which may suggest presence of the antiporter system also at the BCSFB (Figure 6D).

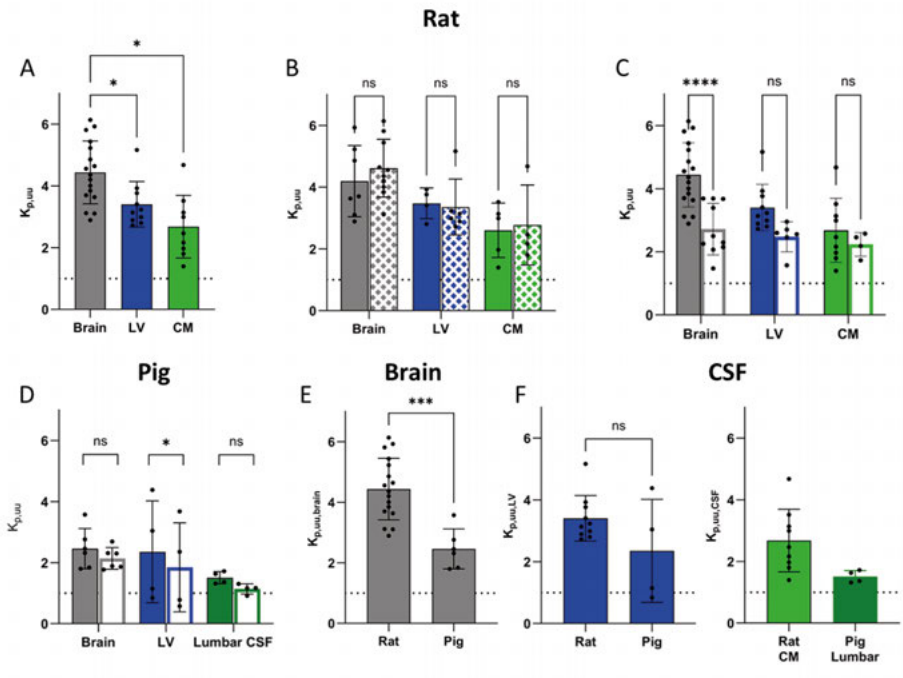

Figure 6. Unbound oxycodone partition coefficients ($K_{p,uu}$) in brain (gray), lateral ventricle (LV, blue), and *cisterna magna* (CM, light green) or lumbar (dark green) cerebrospinal fluid (CSF) in **A**) rats of both sexes, **B**) female (filled) and male (pattern) rats, **C**) healthy (filled) and lipopolysaccharide (LPS)-treated (open) rats, **D**) healthy (filled) and LPS-treated (open) pigs, **E-F**) healthy rats and pigs.

Paper V confirmed active uptake for several antiporter substrates, including oxycodone, pyrilamine, tramadol, bupropion, diphenhydramine, and memantine across the BBB ($K_{p,uu,brain}$ 1.5–2.6) and also across the BSCB ($K_{p,uu,SC}$ 1.2–2.0). Species similarities in oxycodone BSCB uptake were supported by a single spinal cord sample from a pig in Paper III. However, uptake across the rat BCSFB using the CMA-ROI appeared passive, contrasting with findings in Paper I. Methodological differences may contribute to the conflicting results.

Drugs can enter the CNS either via the BBB or the BCSFB, and once inside, they may further distribute between CSF and ISF through exchange mechanisms. For example, as drugs transported across the BBB may move from the ISF to the CSF through bulk flow and diffusion, the origin of drugs detected in the CSF – whether from BBB or BCSFB transport – often remains uncertain. As the extent of ISF-CSF exchange is not fully understood, it is challenging to determine the relative contribution of each CNS barrier to the overall CNS drug exposure *in vivo*. However, the parallel oxycodone concentration-time profiles in ISF and CSF in rats (Paper I), suggest that oxycodone primarily enters the CSF via the BCSFB.

The net uptake of antiporter substrates at CNS barriers may result from a combination of mechanisms, including active influx and possibly efflux transporters. However, oxycodone transport across the BBB likely occurs mainly via the H^+/OC antiporter, as oxycodone has not been identified as a substrate for other BBB influx transporters[62]. Its interaction with the efflux transporter P-gp is debated, as some studies suggest it may act as a P-gp substrate[67, 168, 169], inducer[168], or neither[170]. Yet, the influx is dominating the net transport of oxycodone to the CNS. Antiporter substrates have also been associated with multiple uptake transporters, such as diphenhydramine for OCT1, and memantine for OCT2[62], and pyrilamine for both[171-173]. The substrate's interactions with P-gp vary, for example, pyrilamine has been suggested as a substrate[174] whereas diphenhydramine has not[175]. Such variability in transporter involvement complicates the generalization of transport mechanisms for antiporter substrates and can lead to substrate-specific outcomes.

Utility of CSF as a surrogate for brain ISF concentrations

The microdialysis studies in rats and pigs investigated whether CSF could serve as a reliable surrogate for brain ISF concentrations of actively transported drugs like oxycodone (Papers I and III). These studies compared oxycodone transport across the BBB and BCSFB in both species, with the pig study also assessing drug delivery to the lumbar spine, as it is a common clinical sampling site for CSF. Paper V further examined the transport of multiple antiporter substrates across the barriers using the CMA-ROI method.

In rats, oxycodone transport across the BBB was 46% higher than across the BCSFB (Figure 6A, $p=0.04$), resulting in higher oxycodone concentrations in brain ISF than in CSF. Although CSF measurements underestimated brain ISF concentrations, CSF still revealed the net uptake to CNS. If accepting a threefold variability from ISF, CSF could serve as an indicator of the uptake of an antiporter substrate. The observation of no differences in drug exposure between brain ISF and CSF sites during LPS-induced inflammation in rats supported the use of CSF as a surrogate for ISF (Paper II). However, Paper V showed larger discrepancies between $K_{p,uu,brain}$ and $K_{p,uu,CSF}$ for oxycodone and other antiporter substrates in rats, with predominant passive transport into CSF. This further suggests that CSF may underestimate ISF for these drugs.

In pigs, active uptake of oxycodone across the BCSFB was similar to uptake across the BBB, although substantial variation was observed in the BCSFB transport. The lumbar CSF concentrations were significantly lower than those in the brain ($K_{p,uu,brain} = 2.5$, $K_{p,uu,lumbarCSF} = 1.5$, $p=0.007$), indicating that lumbar CSF underestimates, and thus, may not accurately reflect brain ISF concentrations. Despite this, the mean $K_{p,uu,lumbarCSF}$ still showed net uptake into CSF. In humans, an estimated oxycodone $K_{p,uu,lumbarCSF}$ of around 2, based on plasma protein binding-adjusted total AUC ratios (Paper I), aligned well with pig data (Paper III). This further supports net oxycodone uptake into lum-

bar CSF across species and suggests a good translatability of lumbar CSF exposure between pigs and humans. Hence, although lumbar CSF may not be a suitable surrogate for brain ISF, it may be a reasonable translational tool.

These findings question the quantitative role of CSF as a proxy for ISF but suggest that CSF may serve as a useful indicator of the net CNS transport, aligning with previous conclusions[114, 117, 121]. This has significant impact on CNS drug monitoring. While CSF remains valuable due to its accessibility in humans, if CSF concentrations are lower than expected, dose adjustments should be made with caution.

Impact of inflammation on oxycodone PK and CNS disposition in rats and pigs (Papers II-III)

The impact of LPS-induced inflammation on the systemic PK and CNS drug disposition was studied in rats (Paper II) and pigs (Paper III) using microdialysis. The H^+/OC antiporter system was in focus with oxycodone as a model substrate.

Successful attainment of inflammation in rats and pigs

Studies in both rats and pigs demonstrated that the use of LPS successfully induced systemic inflammation. In rats (Paper II), the LPS challenge elevated inflammatory biomarkers such as IL-6 in both plasma and brain, confirming an immune response. The inflammatory response was more extensive in plasma, with 79 out of the 92 studied biomarkers showing significant elevation compared to only three in the brain. This was further evidenced by the PCA plots of the biomarkers displaying clear separations between healthy and LPS-treated groups in plasma but not in brain. The origin of biomarkers in the brain remains uncertain, but the higher levels observed at the probe site in LPS-treated rats, compared to the contralateral hemisphere, and compared to LPS-treated rats without probes, could suggest a potential plasma origin. This raises the question of possible biomarker leakage across the BBB at the site of probe placement. A previous study using *ex vivo* autoradiography of brain sections from mice intravenously administered with an antibody prior to microdialysis revealed higher antibody delivery at the probe placement site compared to other areas of the brain[176]. The biomarkers studied are large molecules varying in size, for example, human IL-6 typically ranges from 23 to 30 kDa[177] and chemokines are typically smaller, 8–10 kDa[178]. This may suggest BBB impairment in this size range or larger. Yet, the transport of inflammatory biomarkers across the BBB is complex and varies between markers, such as cytokines. For example, IL-6 which may experience increased passive transport, is also actively transported via a saturable system and its CNS exposure is further limited by degradation[179]. Although the absolute extent of

BBB uptake may be limited, it may still be significantly increased during pathological conditions.

Pigs also demonstrated signs of systemic inflammation induced by LPS, as indicated by physiological changes including metabolic acidosis and increased heart rates (Paper III). These findings are consistent with previously reported physiological derangements following LPS challenge in pigs[158, 160, 180, 181]. The pig SOFA scores supported a successful achievement of a sepsis-mimicking state. Similar to our findings in rats, the LPS origin and dose used in Paper III have been documented with elevated levels of cytokines in pigs[159, 160].

LPS is known to affect the immune response in a dose- and time-dependent manner[138, 159], and further, there is evidence suggesting that the route of administration has an impact on the response[182]. While the inflammation model in pigs may induce a more direct response, the model in rats included a larger LPS dose per kg body weight and longer exposure time. Although similar signs of inflammation and CNS drug distribution may be observed, comparing different LPS models is challenging due to likely variations in immune response and inflammation severity. Species differences in LPS response have also been documented. For instance, a study comparing pig and mouse brains following LPS challenge indicates significant differences in gene regulations[183]. Additionally, a study in various mouse strains showed that genetics play a critical role, as demonstrated by significant differences in mortality rates and cytokine responses following LPS challenge[184].

Impaired BBB integrity during inflammation

LPS was documented to compromise BBB integrity in rats (Paper II), demonstrated by an almost sixfold increase in paracellular transport of the 4 kDa dextran. Interestingly, this increased barrier "leakiness" was consistent across the investigated brain regions. Although the largest dextran K_p value was observed at the probe site in LPS-treated rats, it could not be statistically confirmed that probe placement caused the integrity loss. While this effect was reported for antibody brain delivery[176], a higher brain exposure at the probe site may be less pronounced for small molecular drugs due to differences in BBB transport mechanisms and diffusion properties between small and large molecules. Additionally, an impaired BBB integrity following LPS challenge has been reported to occur independently of microdialysis probe placement[185-187]. Yet, some brain regions may be more vulnerable to LPS-induced disruption than others[186]. Despite the compromised barrier, the absolute extent of dextran uptake remained low, with a K_p of 0.29% after LPS treatment. Although these findings were specific to rats, similar alterations of BBB integrity have been documented in pigs under endotoxemia. Previous studies in pigs using biomarkers such as S100B also suggest a compromised BBB, although transient[180, 188], indicating that higher species may experience similar changes during inflammation.

Decreased net uptake of oxycodone during inflammation

In both rats (Paper II) and pigs (Paper III), LPS-induced inflammation reduced the net uptake of oxycodone. In rats, $K_{p,uu,brain}$ decreased to 60%, from 4.4 to 2.72 ($p<0.0001$, Figure 6C). Similarly, in pigs, $C_{u,ss,blood}$ remained stable while $C_{u,ss,brain}$ decreased during inflammation ($p=0.006$), resulting in a reduction of $K_{p,uu,brain}$ from 2.5 to 2.1, although this change did not reach statistical significance (Figure 6D). In the CSF compartments, there was also a trend of decreased uptake by inflammation, both in rats and pigs, although not always reaching significance. A hypothesis emerging from this pig study was that the more severe the inflammation, as determined by scores like SOFA, may lead to a larger reduction in $K_{p,uu}$ of active uptake drugs (Paper III). While this small data set may suggest a potential correlation between higher pig SOFA score and reduced CNS uptake, further studies are required to confirm the relationship between inflammation severity and CNS drug exposure.

Despite the observed reduction in CNS uptake, active net uptake was still preserved in both species, suggesting that the H^+/OC antiporter continues to function at several CNS barriers during inflammation. The mechanism responsible for the reduced uptake remains unclear, as net transport may be influenced by both passive and various active processes. It is uncertain whether the reduced uptake is due to an impaired BBB integrity resulting in an increased passive transport along the concentration gradient, or if involved transporter activities are altered by inflammation. The antiporter uptake may be reduced, or increased as a compensation mechanism for the loss of barrier integrity, although still not reaching the same level of net uptake as in healthy conditions as passive transport is increased. A decreased blood pH, as observed in the pig study (Paper III), may affect the activity of the antiporter as it exchanges a proton for an organic cation. Additionally, oxycodone's potential interaction with P-gp, including potential induction, complicates this further[168, 169]. Previous studies on LPS in mice demonstrated an initial P-gp impairment followed by induction after 36 hours[189]. An induction was also reported following increased levels of the inflammation marker, IL-1β[190], which was elevated both in plasma and brain in our study (Paper II).

Although our studies have demonstrated decreased oxycodone delivery to the CNS across species, questions remain about by which mechanisms inflammation alters CNS barrier transport. Additionally, the timing and duration of these processes require further investigation. If oxycodone transport is similarly reduced during inflammation also in humans, dose adjustments may be necessary to maintain therapeutic efficacy in affected patients.

Sex-dependent systemic PK of oxycodone without impact on the CNS disposition during inflammation

No differences in the extent of oxycodone delivery to the CNS between sexes were found in the studies included in this thesis (Figure 6B), suggesting that

the CNS delivery of oxycodone is sex-independent both in healthy and inflammatory conditions. Similar antiporter function in both sexes further supports the potential of the H^+/OC antiporter system as a promising mechanism for targeted CNS drug delivery in humans.

While our data indicate no sex-dependent differences in the systemic PK in healthy rats and pigs (Papers I and III), the unbound oxycodone exposure (AUC) in blood was larger in LPS-treated females compared with LPS-treated males, as well as healthy females, due to a sex-specific reduction in clearance caused by LPS (Paper II). This may be related to a sex-specific effect of inflammation on oxycodone metabolizing enzymes. Oxycodone is mainly metabolized, with the key enzymes being CYP3A4 and CYP2D6[191-193]. The previously reported sex-dependent differences in oxycodone brain exposure across different phases of the estrous cycle[85] were attributed to variations in CYP2D-mediated brain metabolism of oxycodone, yet in healthy rats. In addition, inflammation is known to impact metabolizing enzymes. In a human liver spheroid model incubated with IL-1β, IL-6, or TNF-α, significant reductions in mRNA expression of CYP3A4, and to a lesser extent also CYP2D6, were observed[194]. Although this was beyond the scope of our studies, our findings highlight that sex-specific functions of metabolizing enzymes, particularly under inflammatory conditions, are complex processes that require further investigation.

Species variations in oxycodone CNS disposition and systemic PK (Papers I and III)

The microdialysis studies in rats and pigs revealed species variations in oxycodone CNS disposition and systemic PK. Both studies demonstrated active transport across the BBB and the BCSFB (Figure 6). However, $K_{p,uu,brain}$ was approximately 1.8-fold lower in pigs compared to rats ($p=0.0002$, Figure 6E), which may suggest species-related variations in transporter expression or function at the BBB. No significant species difference was observed in the BCSFB uptake ($K_{p,uu,LV}$, Figure 6F). Hence, the findings support the hypothesis of a preserved H^+/OC antiporter system across species but also highlight the importance of considering species variations in the CNS drug disposition.

The complexity of oxycodone's net transport may be influenced by species differences not only in antiporter function, but in multiple transport pathways, including the possible interaction with P-gp, or differences in passive transport. For instance, studies have shown lower P-gp activity in higher species[86, 87], and lower protein expression in humans compared to rats[195] with pigs showing similar levels as humans[196]. However, if uptake is similar but efflux

is lower in pigs, a higher net uptake in pigs compared to rats would be expected, which was not observed in our studies. This may suggest that antiporter-mediated uptake is also lower in pigs.

The unbound oxycodone plasma clearance was around fourfold higher in rats than in pigs (101 versus 23 mL/min/kg, $p < 0.0001$). This indicates slower systemic clearance in higher species, which aligns with a human study reporting a total plasma clearance of around 11.5 mL/min/kg[197]. The observed differences may be due to species differences in the activity of metabolizing enzymes. Studies on human, pig, and rat microsomes revealed similar CYP3A4 activity, but faster CYP2D6 activity in pig and rat compared to human material[198-200], which likely contributes to the observed species differences in oxycodone clearance. These findings highlight the importance of considering species-specific variations in both systemic PK and CNS barrier transport when extrapolating preclinical data to humans.

Oxycodone and ^{3}H-pyrilamine uptake in *in vitro* BBB models (Paper IV)

In Paper IV, the functionality of the H^+/OC antiporter system in BBB cell models from various species, and their correlation with *in vivo* data, was explored. Drug uptake was assessed in human hCMEC/D3 cells and primary rat BECs, with pilot studies also conducted in mouse and pig BECs, using oxycodone and ^{3}H-pyrilamine as model substrates. Cellular uptake was observed in hCMEC/D3 and primary BECs, and transport was observed across all BEC models.

The uptake kinetics in hCMEC/D3 suggested a saturated uptake mechanism, likely mediated by the H^+/OC antiporter. The oxycodone $K_{p,uu,cell}$ in hCMEC/D3 was 1.7±0.3 across different oxycodone concentrations and incubation times, showing a high capacity and rapid uptake by the system. Oxycodone uptake into mouse and rat BEC could not be assessed due to cell sample concentrations below LLOQ. Still, in the pig BEC model, oxycodone $K_{p,u,cell}$ was 31 (n=2). Applying an $f_{u,cell}$ similar to that of 10.5% determined in hCMEC/D3 would result in an oxycodone pig BEC $K_{p,uu,cell}$ above unity. The ^{3}H-pyrilamine $K_{p,u,cell}$ in rat BECs was 38.5±22.4, suggesting intracellular accumulation.

Oxycodone active uptake across rat and pig BEC models was supported by ER of 0.4 and 0.6, resulting in $K_{p,uu,brain}$ values of 2.4 and 1.7, respectively. These values align well with *in vivo* data from rats and pigs (Papers I and III, Figure 6), although slightly lower, indicating that these models could be valuable tools for the identification of net uptake. However, these permeabilities were not corrected for contributions from the unstirred water layer and Transwell insert[201-203]. These corrections are crucial to obtain the permeability of the BEC layer.

The rat BEC study, together with the pilot experiments in mouse and pig BEC models, reveal a less than twofold variability in the apparent permeability of oxycodone A→B (Figure 7), suggesting small differences in transporter function across BEC origins. Also here, these are system-specific permeability values, without correction for contributions from the unstirred water layer and the insert. Yet, as the same stirring conditions and inserts were used for all BEC transport studies, the correction would impact values across all BEC origins similarly.

Despite similar transport across BEC of different origins, TEER values varied significantly with mean TEER values of 382±64 Ω×cm^2 (mouse), 40±24 Ω×cm^2 (rat), and 644±195 Ω×cm^2 (pig). This trend of higher TEER across pig BECs compared with rodent BECs has previously been documented[204]. As TEER is considered to reflect barrier tightness, pig BECs appear to form a tighter barrier than rodent models. Nonetheless, despite these differences, the models have previously been documented to exhibit similar impermeability to ^{3}H-D-Mannitol, used as a barrier integrity marker. The differences in TEER was attributed to variations in cell sizes across species[204].

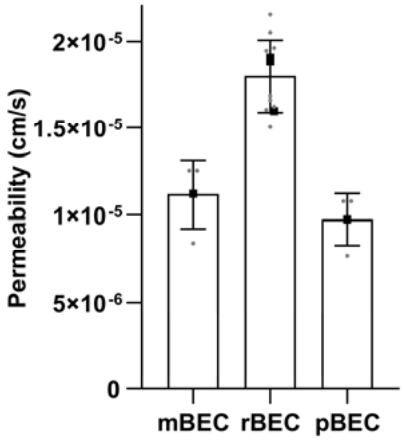

Figure 7. Apparent permeability of oxycodone across mouse (m), rat (r) and pig (p) brain endothelial cell (BEC) in *in vitro* Transwell models from the apical to the basolateral compartments. Batch mean values are indicated by black squares and technical replicates by gray dots. The top of the bar represents the mean and error bars the SD.

In hCMEC/D3 cells, IL-6 treatment enhanced the extent of oxycodone uptake, suggesting that the cytokine influence drug uptake into these cells. However, this contrasts with *in vivo* observations during inflammation, where a trend of reduced BBB uptake was observed (Papers II–III). The difference between the *in vitro* and *in vivo* results underscores the complexity of *in vivo* immune responses, highlighting the limitations of using individual cytokine treatments as general models for inflammation. Cytokine treatments in various *in vitro* models have shown scattered effects on transporter function and expression levels, with both increasing[190, 205] and decreasing[206] effects on efflux transporters, as well as increasing[207] and decreasing[208] effects on influx transporters. IL-6 may promote oxycodone uptake through several mechanisms, such as enhancing antiporter-mediated uptake, reducing possible P-gp-mediated efflux, or affecting the pH gradient to favor pH partitioning of organic cations.

The latter is supported by a previous study of IL-6-treated dendritic cells, showing an acidification of early endosomes[209]. If extended to other cell types, this may contribute to an increased extent of organic cation trapping also in endothelial cells. If IL-6 similarly increases the uptake of antiporter substrates *in vivo*, additional mechanisms, such as loss of BBB integrity, likely counteract this effect during inflammation.

These findings highlight the importance of selecting appropriate *in vitro* models for studying BBB transport to accurately predict *in vivo* CNS drug transport, which is crucial in CNS drug development. In terms of characterizing active uptake of antiporter substrates, the human hCMEC/D3 as well as mouse, rat and pig BEC model have demonstrated reliability, aligning with *in vivo* conclusions. However, for studying complex systems like immune responses, it is essential to complement *in vitro* studies with *in vivo* data to fully capture the biological complexity.

$K_{p,uu,cell}$ as a key metric for comparing drug transport across experimental models

Studies in Papers IV–V focus on the transport of oxycodone and other antiporter substrates into brain endothelial and parenchymal cells, comparing active uptake mechanisms between cell types and experimental models. In Paper IV, oxycodone's active uptake was demonstrated in both endothelial cells (hCMEC/D3) and brain parenchymal cells. Despite variations in the extent of cellular oxycodone accumulation (assessed by $K_{p,u,cell}$ and $V_{u,brain}$) due to differences in binding properties, the consistent net uptake was revealed by $K_{p,uu,cell}$ values of 1.7–1.9 in both cell types.

In Paper V, this approach was further extended by using $K_{p,uu,cell}$ to evaluate the intracellular distribution of various antiporter substrates within brain parenchymal cells. Despite of an almost tenfold difference in $V_{u,brain}$ between substrates, observed $K_{p,uu,cell}$ values ranged from 1.6 to 3.1. This reflects the differences in binding properties and indicate similar intracellular accumulation between substrates, further demonstrating the valuable use of $K_{p,uu,cell}$ for assessment of the intracellular unbound drug exposure.

As previously described, $K_{p,uu,cell}$ is also valuable as it can be used to distinguish between uptake processes by predicting $K_{p,uu,cell}$ using the pH partitioning model[75]. The pH partitioning model accounts for uptake driven solely by pH differences between plasma, cytosol, and lysosomes, without taking active transport mechanisms into account. A higher-than-unity predicted value indicates that pH partitioning plays a role for the intracellular drug accumulation, as is the case for oxycodone.

Together, these findings emphasize the importance of $K_{p,uu,cell}$ as a harmonized tool for understanding and comparing drug transport across methods and

cell types. It is also useful for an increased understanding of the role of active transport and pH partitioning in drug transport.

Regional-independent net uptake of H^+/OC antiporter substrates (Paper V)

The studies in Paper V explored the regional CNS distribution of H^+/OC antiporter substrates, revealing $K_{p,uu,ROI}$ values consistently exceeding unity across different brain regions and spinal cord. This indicates region-independent active net uptake of antiporter substrates. Furthermore, intracellular drug accumulation in parenchymal cells was observed for all substrates, with $K_{p,uu,cell}$ values above 1.6. Consistently higher-than-unity $K_{p,uu,ROI}$ and $K_{p,uu,cell}$ values across CNS regions at clinically relevant plasma concentrations may contribute to high extra- and intracellular drug exposure. High CNS exposure of antiporter substrates may contribute to the clinically reported drug-induced neurotoxic effects, such as seizures and cognitive impairments. However, the observed minor differences in drug exposure between regions may be attributed to regional variations in the expression of P-gp and the junctional protein Claudin-5[31, 210], without differences in antiporter-mediated uptake. As the extent of drug accumulation was highly sensitive to pH changes, pathological conditions with an increased pH gradient in the brain may increase the risk of drug-induced neurotoxicity. The findings from this study highlight the importance of comprehensive neuroPK assessments in CNS drug development to evaluate the risk of drug-induced CNS adverse events.

Mechanisms driving CNS disposition of H^+/OC antiporter substrates (Papers IV–V)

While there is *in vivo* evidence of an active net uptake of antiporter substrates across the BBB (Papers I-III), there are also findings suggesting that other mechanisms, such as pH partitioning, play a role in the CNS disposition of these drugs. Paper IV confirmed the active net uptake of oxycodone into both brain endothelial and parenchymal cells. Paper V explored the roles of active transport and lysosomal trapping, showing minimal differences between observed (1.6–3.1) and predicted (2.8 for all substrates) $K_{p,uu,cell}$ values, highlighting the role of pH partitioning, including lysosomal trapping, in intracellular accumulation. The pH dependency was further confirmed by reduced uptake in the presence of pH modulators like monensin and bafilomycin A, which increase lysosomal pH. However, these experiments affect both pH partitioning and the pH-dependent antiporter, making it difficult to distinguish between the two processes, underscoring the complexity of these interactions. A saturable uptake mechanism was confirmed by Michaelis-Menten kinetics.

While the concept of saturation applies to transport systems like the H^+/OC antiporter, lysosomal trapping may also become saturated. This phenomenon has previously been documented, for example in rat hepatocytes with basic lipophilic compounds, such as propranolol, showing drug-specific half-maximal inhibitory concentration (IC_{50}) values[211]. This further adds complexity to differentiate between the active and lysosomal trapping components in antiporter substrate transport mechanisms.

Evidence supporting the presence of active transport of antiporter substrates in addition to the lysosomal trapping, is that not all organic cations are antiporter substrates[71]. Although TM7SF3 and LHFPL6 have been identified as key components of the antiporter system[78], neither protein appears to be associated with pH regulation, raising questions about their endogenous role in this process. Despite this, these proteins do not appear to fully account for the antiporter-mediated uptake, suggesting that additional components of the antiporter system remain to be identified. Furthermore, lysosomal active influx and efflux mechanisms mediated by the H^+/OC antiporter and SLC49A4, respectively, have been proposed[212], adding complexity to the understanding of CNS drug distribution.

These findings emphasize the critical role of pH partitioning in the brain disposition of antiporter substrates, and likely other organic cations, without rejecting the active uptake component. The dual pH dependence of the H^+/OC antiporter and lysosomal trapping complicates the distinction between active and passive transport mechanisms. This underscores the need for further research to clarify the contributions of these mechanisms to CNS drug delivery to aid the development of effective and safe CNS-targeted therapies.

Conclusions

The main focus of this thesis was to explore the function of the H^+/OC antiporter to obtain brain-specific drug delivery. Various translational aspects have been addressed, using both *in vivo* and *in vitro* models. The overall aim has been to increase the understanding of active drug uptake across CNS barriers and to explore methods to study brain drug delivery, to overcome the high failure rate due to inadequate drug target-site exposure and safety concerns in CNS drug development.

The studies presented in this thesis collectively demonstrate significant advancements in understanding CNS drug disposition of H^+/OC antiporter substrates. The findings confirm active uptake across various CNS barriers in both rats and pigs, with only minor inter-species variations. This supports the potential of targeting this system for CNS drug delivery in humans. While sex-dependent differences may occur in the systemic PK of antiporter substrates, the CNS drug delivery mechanism is stable across sexes, further highlighting its usage potential. Although an active uptake component is evidently present, pH partitioning appears to play a critical role in brain accumulation of antiporter substrates. The studies also emphasize the complexities associated with pathologies, such as inflammation, showing that LPS-induced inflammation can impact both systemic pharmacokinetics and CNS drug delivery, resulting in reduced CNS exposure. However, the underlying mechanisms of reduced uptake remain to be fully understood. The high CNS delivery of antiporter substrates across brain regions, along with previous reports on the association with neurotoxicity, underscores the necessity for careful evaluation of CNS-targeted therapies to ensure safety and efficacy.

In vitro BBB models from various origins can provide valuable insights in brain drug delivery and show promise for verification of uptake mechanisms. Yet, translating these findings directly to *in vivo* conditions, particularly under pathological states, still have limitations, highlighting the need to complement *in vitro* data with *in vivo* studies for a more comprehensive understanding of drug uptake.

Populärvetenskaplig sammanfattning på svenska

Hjärnan är ett komplext organ som styr många av kroppens funktioner. För att skydda hjärnan finns barriärer, framförallt blod-hjärnbarriären, som reglerar vilka molekyler, inklusive läkemedel, som kan passera in. Hjärnans barriärer är utrustade med både sammanfogande proteiner, som gör att upptaget mellan celler i barriären begränsas kraftigt, och transportproteiner som antingen kan hindra eller främja molekylers inträde i hjärnan. Vissa av upptagstransportörerna kan potentiellt användas för att specifikt leverera läkemedel till hjärnan, vilket kan leda till säkrare och mer effektiva behandlingar. En av dessa lovande transportörer är den protonkopplade organiska katjon-antiportern (H^+/OC antiportern), som visat sig effektivt ta upp vissa läkemedel så som oxikodon och pyrilamin till hjärnan. Trots det återstår många frågor innan denna transportör kan utnyttjas fullt ut i läkemedelsutvecklingen.

Hos människor mäts upptaget till hjärnan sällan genom att ta prover från hjärnan. En vanligare metod för att uppskatta läkemedelsnivåer i hjärnan är att ta prover från cerebrospinalvätskan i ryggmärgen. Det är dock oklart om denna vätska exakt speglar läkemedelsnivåerna i hjärnvävnaden. Andra metoder som används för att uppskatta läkemedelsnivåer i hjärnan hos människor är att undersöka hur det ser ut i försöksdjur, eller till och med i celler som speglar blod-hjärnbarriären. Dessa djur- och cellmodeller överensstämmer inte alltid med effekten hos människor, vilket försvårar prediktionerna. Andra utmaningar inom läkemedelsutveckling för hjärnans sjukdomar ligger också i att läkemedel ofta inte når tillräckligt höga nivåer i hjärnan. Därför behöver vi bättre förstå omfattningen av upptaget, och skillnaderna mellan arter men även mellan män och kvinnor, då transportörers funktion kan variera beroende på art och kön. Dessutom kan sjukdomstillstånd, som inflammation, förändra transportörernas aktivitet och därmed påverka läkemedelsleveransen till hjärnan. Eftersom inflammation är ett vanligt tillstånd som finns vid olika sjukdomar, inklusive hjärnans sjukdomar, är det viktigt att veta hur läkemedelsleveransen till hjärnan via H^+/OC antiportern påverkas av inflammation.

Forskningen som presenteras i den här avhandlingen visar att upptaget av bland annat oxikodon och pyrilamin via antiportersystemet fungerar både i friska och inflammerade hjärnor hos djur, trots ett minskat upptag under inflammation. Små variationer i läkemedelsupptaget observerades mellan råttor och grisar medan ingen skillnad observerades mellan könen. Försöken indike-

rade också att ryggmärgsvätska inte alltid speglar läkemedelsnivåerna i hjärnan, vilket är viktigt att veta eftersom det kan ha betydelse för hur dosen av läkemedel justeras under en behandling. Studierna visade också att cellmodeller kan vara lovande verktyg att använda för att tidigt identifiera vilka läkemedel som har störst potential att tas upp i hjärnan, vilket skulle kunna effektivisera utvecklingsprocessen av läkemedel. Sammanfattningsvis har denna avhandling undersökt hur antiportersystemet kan användas för att leverera läkemedel till hjärnan, samt hur dess funktion kan variera mellan arter, kön och vid sjukdomstillstånd, i försöksdjur och cellmodeller. Trots att mer forskning krävs för att förstå antiporterns fulla potential pekar resultaten på att den är en lovande strategi för att förbättra specifik läkemedelsleverans till hjärnan och behandla dess sjukdomar.

Acknowledgements

The research presented in this thesis was primarily conducted at the Department of Pharmacy and the Department of Public Health and Caring Sciences at Uppsala University (Sweden). Individual projects were carried out in collaboration with the the Department of Surgical Sciences at Uppsala University (Sweden), the Department of Pharmacy at the University of Copenhagen (Denmark), and the Department of Biomedicine at Aarhus University (Denmark).

I gratefully acknowledge the financial support provided by the Swedish Research Council (Vetenskapsrådet, grant no. 2018–03310), Innovative Medicines Initiative 2 Joint Undertaking projects IM2PACT (grant no. 807015, 2019) and NeuroDeRisk (grant no. 821528, 2019). The Joint Undertaking receives support from the European Union's Horizon 2020 research and innovation programme and EFPIA. Additionally, I would like to thank the Swedish Academy of Pharmaceutical Sciences (Apotekarsocieteten), including IF's Stiftelse and Källrotsstipendiet, ULLA European University Consortium for Pharmaceutical Sciences, and Anna-Maria Lundin's Foundation at Smålands Nation, for funding research visits and participation in conferences.

I would like to express my deepest gratitude to everyone who has supported me throughout my PhD journey! This work would not have been possible without the guidance, encouragement, and generosity of many incredible people. Special thanks to:

My main supervisor, **Irena Loryan**. Thanks for accepting me as your first (main) PhD student and for always believing in me. Your unwavering support, scientific expertise, and dedication have been invaluable. I deeply appreciate all our nitty-gritty discussions, your willingness to step into the lab whenever needed, and your patience. Thanks for introducing me to amazing researchers in the BBB community, continuously challenging me to grow, and welcoming me with open arms whenever I knock on your door – regardless if it is with tears or laughter (or maybe a bottle of champagne).

My co-supervisor, **Margareta Hammarlund-Udenaes**. Thanks for always hanging around – for always making time to discuss research (or anything else), whenever I have questions. Your honesty, generosity, and kindness have meant a lot to me, as have our fun times together. I am very grateful for all your support, our conceptual discussions and manuscript meetings.

My co-supervisor, **Stina Syvänen**. Thanks for your all your support and for always making me feel like I could turn to you when I needed help. Thanks

for always being generous with your time, whether explaining things, reading drafts, engaging in discussions, or mental support. Thanks for making me feel comfortable whenever I need it and for asking me "what is the worst thing that can happen". Och tack för alla grisiga dagar på lab!

All past and present members and visitors of the **Translational PKPD group** for great research, discussions and a lot of fun! Especially: **Jessica**, stort tack för all hjälp inför och under experiment, och för allt tok och alla skratt! **Aghavni, Milda and Canan** – my PhD journey would not have been the same without you, thanks for your support and a lot of goofy business. **Erik** – my big brother in research, you were the best mentor! Thanks for all our talks about research, and anything else in life. **Yang –** for being there in the beginning and always explaining and helping me whenever I needed it, for coming to BMC on a Saturday when I needed help with the MS, for fun driving sessions, for wall sits in the lab, and more. **Markus –** although far away, very present. Thanks for making time to teach me concepts of modelling, for challenging me, and questioning me regarding the existence of the antiporter, and other discussions during these years.

My fantastic collaborators and co-authors, without your contributions and dedication, these projects would not have turned out as good as they did. Especially: **Birger Brodin** at the University of Copenhagen – Thank you for insightful knowledge exchange and conceptual discussions, and for warmly welcoming me into your group. You really made me feel like home. **Miklós Lipcsey** at Uppsala University – Thank you for accepting our invitation to be a vital part of the project, and your enthusiastic involvement and positivity, and for always being available to answer my questions. **Morten Schallburg Nielsen** at Aarhus University – Thank you for joining our project without hesitation, despite the short time line over summer vacations, and for great conceptual discussions. **Liesbeth de Lange** at Leiden University – Thank you for all the engaging and insightful discussions during the years, and for inviting us to your lab. I am happy to finally call you a collaborator.

All members of the **CNS Drug Delivery and Barrier Modelling group** (University of Copenhagen) for really adopting me as a PhD student in your group and always being kind and helpful. Mange tak! Especially: **Mie**, thanks for your support and positivity. **Nana, Alberte, Kristine**, and visiting **Vilém**, thanks for all your invaluable help and fun times both within and outside the lab. **Burak**, for teaching me so much during my first visit, and for letting me borrow your desk.

Hedenstierna staff, for opening up the world of GRIVA and over and over explaining readouts and technical equipment to me, and convincing me that 1 mL is not a big sample volume.

Annemette at Aarhus University for performing cell experiments on demand and immediately answering all my (many) email questions. Without your experiments I would have learned a lot less.

My master students throughout these years, for all your great contributions and all the fun we have had: **Tilda, Jessica, Shannuo** and **Jaquline**.

All amazing PhD students in the pharmacometrics groups, for your complex presentations, interesting discussions and laughter through the years (some of you even became my modelling teachers!). Especially: **Viktor, Haini, Han, Hanna, Alan, Rami, Eman, Salma, Maddalena, Raphaël, Amaury, Romain, Mohamed** and **Zhe**.

ProDDe and Immune oncology groups. The B3:4 floor has felt so much more alive since you moved in. Special thanks to **Nicole, Ana** and **Inga** for great fun and for including us in your singing practices, and more.

All past and present **teachers in pharmacokinetics and pharmacotherapy**, for your dedication and for guiding me as a teacher. Special thanks to **Jörgen**, for being my rock in teaching: for your support and for always believing in me. Thanks to my **PhD teaching colleagues** for being a great team and making teaching sessions even more fun.

All fantastic PhD students I got the opportunity to meet via **FDR** and **AAPS**. Thanks for making a difference for PhD students and for contributing to such a great community.

Friends and colleagues at the department, for creating such a nice work environment, for insightful discussions, and for all the small kitchen chitchats. It means a lot.

Fanny L, for always being there for me, trough the good and the tough times. Thanks for drawing a map of BMC so I could study the building before starting as a student, for sharing notes, tips and tricks throughout our studies and PhD journeys. **Malin**, for encouraging me to apply for this PhD position and practicing the interview with me – Tada, here is the result! I will also always cherish the fun times we have had over the years, especially your unforgettable parties at Väktargatan. **Jenny N**, for being such a great friend, for always caring, and bringing so much fun into my life. You are truly a ray of sunshine! **Rosita**, my better twin sister, for all the fun moments, but also for our discussions and the exchange of ideas and experiences. **Merve**, for always inviting me to hang out! Thanks for always being fun and positive, and for all our supportive talks.

Mina apotekar-gals, **Helga, Lidia, Michaela, Julia**, för alla stunder tillsammans genom åren: plugg, skratt, gråt, skratt-gråt, utekvällar, cykelresor till Glöte, nattågsresor, och allt däremellan. Tack för att ni alltid har funnits där, er pepp har betytt mycket! **Gucci gang**, för allt bus och för att ni alltid får mig att glömma stressiga dagar. **Bokvincirkeln** för att ni fått mig att läsa annat än vetenskapliga artiklar, även om jag tycker att det varit lite dåligt med vin! **Sandviken gang**, för att ni är så nära fast ni är långt borta. Tack för alla skratt, Snapchat-gossip och att ni finns där för mig!

Fröknarna på **Ashtanga yoga Uppsala** och **Fredrik**, jag tror inte att ni förstår hur mycket ni bidragit till den här avhandlingen. Utan er hade det inte gått.

Fanny, mamma och **pappa**, ni betyder så mycket för mig! Tack för att ni alltid finns där och för er villkorslösa kärlek. För att ni alltid svarar oavsett när jag ringer. Vad skulle jag göra utan er? Tack till **bonusföräldrar, mor- och**

farföräldrar, Victor (och hallonet), **min bonusfamilj Samuelsson-Renglund** och övriga familjen för att ni alltid ger mig en plats där jag kan landa och bara vara Frida.

John, mitt livs kärlek. Tack för att du finns hos mig! Utan dig hade den här resan inte blivit densamma. Jag älskar att komma hem för jag vet att du är där, och det gör mig så glad. Jag ser fram emot vår framtid tillsammans!

Frida

Uppsala, October 2024

References

1. Talevi A, Bellera CL, Di Ianni M, Gantner M, Bruno-Blanch LE, Castro EA. CNS drug development - lost in translation? Mini Rev Med Chem. 2012;12(10):959-70.DOI: 10.2174/138955712802762356.
2. Dowden H, Munro J. Trends in clinical success rates and therapeutic focus. Nature reviews Drug discovery. 2019;18(7):495-6.DOI: 10.1038/d41573-019-00074-z.
3. Kesselheim AS, Hwang TJ, Franklin JM. Two decades of new drug development for central nervous system disorders. Nature reviews Drug discovery. 2015;14(12):815-6.DOI: 10.1038/nrd4793.
4. Butlen-Ducuing F, Pétavy F, Guizzaro L, Zienowicz M, Haas M, Alteri E, Salmonson T, Corruble E. Regulatory watch: Challenges in drug development for central nervous system disorders: a European Medicines Agency perspective. Nature reviews Drug discovery. 2016;15(12):813-4.DOI: 10.1038/nrd.2016.237.
5. Gribkoff VK, Kaczmarek LK. The need for new approaches in CNS drug discovery: Why drugs have failed, and what can be done to improve outcomes. Neuropharmacology. 2017;120:11-9.DOI: 10.1016/j.neuropharm.2016.03.021.
6. Hammarlund-Udenaes M, De Lange E, Thorne R. Drug Delivery to the Brain: Physiological Concepts, Methodologies and Approaches. 2 ed. Perrie Y, editor2022.
7. Abbott NJ, Patabendige AA, Dolman DE, Yusof SR, Begley DJ. Structure and function of the blood-brain barrier. Neurobiol Dis. 2010;37(1):13-25.DOI: 10.1016/j.nbd.2009.07.030.
8. Erickson MA, Dohi K, Banks WA. Neuroinflammation: a common pathway in CNS diseases as mediated at the blood-brain barrier. Neuroimmunomodulation. 2012;19(2):121-30.DOI: 10.1159/000330247.
9. Reese TS, Karnovsky MJ. Fine structural localization of a blood-brain barrier to exogenous peroxidase. J Cell Biol. 1967;34(1):207-17.DOI: 10.1083/jcb.34.1.207.
10. Becker NH, Novikoff AB, Zimmerman HM. Fine structure observations of the uptake of intravenously injected peroxidase by the rat choroid plexus. J Histochem Cytochem. 1967;15(3):160-5.DOI: 10.1177/15.3.160.
11. Abbott NJ, Rönnbäck L, Hansson E. Astrocyte-endothelial interactions at the blood-brain barrier. Nature reviews Neuroscience. 2006;7(1):41-53.DOI: 10.1038/nrn1824.
12. Bartanusz V, Jezova D, Alajajian B, Digicaylioglu M. The blood-spinal cord barrier: morphology and clinical implications. Ann Neurol. 2011;70(2):194-206.DOI: 10.1002/ana.22421.

13. Loryan I, Melander E, Svensson M, Payan M, König F, Jansson B, Hammarlund-Udenaes M. In-depth neuropharmacokinetic analysis of antipsychotics based on a novel approach to estimate unbound target-site concentration in CNS regions: link to spatial receptor occupancy. Molecular psychiatry. 2016;21(11):1527-36.DOI: 10.1038/mp.2015.229.
14. Ge S, Pachter JS. Isolation and culture of microvascular endothelial cells from murine spinal cord. Journal of neuroimmunology. 2006;177(1-2):209-14.DOI: 10.1016/j.jneuroim.2006.05.012.
15. Abbott NJ, Pizzo ME, Preston JE, Janigro D, Thorne RG. The role of brain barriers in fluid movement in the CNS: is there a 'glymphatic' system? Acta neuropathologica. 2018;135(3):387-407.DOI: 10.1007/s00401-018-1812-4.
16. Syková E, Nicholson C. Diffusion in brain extracellular space. Physiol Rev. 2008;88(4):1277-340.DOI: 10.1152/physrev.00027.2007.
17. Abbott NJ. Evidence for bulk flow of brain interstitial fluid: significance for physiology and pathology. Neurochem Int. 2004;45(4):545-52.DOI: 10.1016/j.neuint.2003.11.006.
18. Alimajstorovic Z, Pascual-Baixauli E, Hawkes CA, Sharrack B, Loughlin AJ, Romero IA, Preston JE. Cerebrospinal fluid dynamics modulation by diet and cytokines in rats. Fluids and barriers of the CNS. 2020;17(1):10.DOI: 10.1186/s12987-020-0168-z.
19. Rubin RC, Henderson ES, Ommaya AK, Walker MD, Rall DP. The Production of Cerebrospinal Fluid in Man and Its Modification by Acetazolamide. Journal of Neurosurgery. 1966;25(4):430-6.DOI: 10.3171/jns.1966.25.4.0430.
20. Olav Sand ØVS, Egil Haug. Människans fysiologi: Liber; 2004 2004-08-20.
21. Shetty AK, Zanirati G. The Interstitial System of the Brain in Health and Disease. Aging Dis. 2020;11(1):200-11.DOI: 10.14336/ad.2020.0103.
22. Cserr HF, Cooper DN, Milhorat TH. Flow of cerebral interstitial fluid as indicated by the removal of extracellular markers from rat caudate nucleus. Experimental Eye Research. 1977;25:461-73.DOI: https://doi.org/10.1016/S0014-4835(77)80041-9.
23. Wåhlin A, Ambarki K, Hauksson J, Birgander R, Malm J, Eklund A. Phase contrast MRI quantification of pulsatile volumes of brain arteries, veins, and cerebrospinal fluids compartments: Repeatability and physiological interactions. Journal of Magnetic Resonance Imaging. 2012;35(5):1055-62.DOI: https://doi.org/10.1002/jmri.23527.
24. Yamada S, Miyazaki M, Yamashita Y, Ouyang C, Yui M, Nakahashi M, Shimizu S, Aoki I, Morohoshi Y, McComb JG. Influence of respiration on cerebrospinal fluid movement using magnetic resonance spin labeling. Fluids and barriers of the CNS. 2013;10(1):36.DOI: 10.1186/2045-8118-10-36.
25. Mestre H, Tithof J, Du T, Song W, Peng W, Sweeney AM, Olveda G, Thomas JH, Nedergaard M, Kelley DH. Flow of cerebrospinal fluid is driven by arterial pulsations and is reduced in hypertension. Nature communications. 2018;9(1):4878.DOI: 10.1038/s41467-018-07318-3.
26. Klarica M, Orešković D. Enigma of cerebrospinal fluid dynamics. Croat Med J. 2014;55(4):287-90.DOI: 10.3325/cmj.2014.55.287.
27. Iliff JJ, Wang M, Liao Y, Plogg BA, Peng W, Gundersen GA, Benveniste H, Vates GE, Deane R, Goldman SA, Nagelhus EA, Nedergaard M. A paravascular pathway facilitates CSF flow through the brain parenchyma and the clearance of interstitial solutes, including amyloid beta. Science translational medicine. 2012;4(147):147ra11.DOI: 10.1126/scitranslmed.3003748.

28. Hannocks M-J, Pizzo ME, Huppert J, Deshpande T, Abbott NJ, Thorne RG, Sorokin L. Molecular characterization of perivascular drainage pathways in the murine brain. Journal of Cerebral Blood Flow & Metabolism. 2018;38(4):669-86.DOI: 10.1177/0271678x17749689.
29. Sweet DH. Organic Cation Transporter Expression and Function in the CNS. In: Daws LC, editor. Organic Cation Transporters in the Central Nervous System. Cham: Springer International Publishing; 2021. p. 41-80.
30. Hartz AM, Bauer B. ABC transporters in the CNS - an inventory. Curr Pharm Biotechnol. 2011;12(4):656-73.DOI: 10.2174/138920111795164020.
31. Braun C, Sakamoto A, Fuchs H, Ishiguro N, Suzuki S, Cui Y, Klinder K, Watanabe M, Terasaki T, Sauer A. Quantification of Transporter and Receptor Proteins in Dog Brain Capillaries and Choroid Plexus: Relevance for the Distribution in Brain and CSF of Selected BCRP and P-gp Substrates. Molecular pharmaceutics. 2017;14(10):3436-47.DOI: 10.1021/acs.molpharmaceut.7b00449.
32. Morris ME, Rodriguez-Cruz V, Felmlee MA. SLC and ABC Transporters: Expression, Localization, and Species Differences at the Blood-Brain and the Blood-Cerebrospinal Fluid Barriers. The AAPS journal. 2017;19(5):1317-31.DOI: 10.1208/s12248-017-0110-8.
33. Mastorakos P, McGavern D. The anatomy and immunology of vasculature in the central nervous system. Science immunology. 2019;4(37).DOI: 10.1126/sciimmunol.aav0492.
34. Hammarlund-Udenaes M, Bredberg U, Fridén M. Methodologies to assess brain drug delivery in lead optimization. Current topics in medicinal chemistry. 2009;9(2):148-62.DOI: 10.2174/156802609787521607.
35. Uchida Y, Ohtsuki S, Katsukura Y, Ikeda C, Suzuki T, Kamiie J, Terasaki T. Quantitative targeted absolute proteomics of human blood-brain barrier transporters and receptors. Journal of neurochemistry. 2011;117(2):333-45.DOI: 10.1111/j.1471-4159.2011.07208.x.
36. Al Rihani SB, Darakjian LI, Deodhar M, Dow P, Turgeon J, Michaud V. Disease-Induced Modulation of Drug Transporters at the Blood–Brain Barrier Level. International Journal of Molecular Sciences. 2021;22(7):3742.DOI.
37. Yamazaki Y, Kanekiyo T. Blood-Brain Barrier Dysfunction and the Pathogenesis of Alzheimer's Disease. Int J Mol Sci. 2017;18(9).DOI: 10.3390/ijms18091965.
38. Sweeney MD, Sagare AP, Zlokovic BV. Blood-brain barrier breakdown in Alzheimer disease and other neurodegenerative disorders. Nature reviews Neurology. 2018;14(3):133-50.DOI: 10.1038/nrneurol.2017.188.
39. Al-Bachari S, Naish JH, Parker GJM, Emsley HCA, Parkes LM. Blood-Brain Barrier Leakage Is Increased in Parkinson's Disease. Frontiers in physiology. 2020;11:593026.DOI: 10.3389/fphys.2020.593026.
40. Ortiz GG, Pacheco-Moisés FP, Macías-Islas M, Flores-Alvarado LJ, Mireles-Ramírez MA, González-Renovato ED, Hernández-Navarro VE, Sánchez-López AL, Alatorre-Jiménez MA. Role of the blood-brain barrier in multiple sclerosis. Arch Med Res. 2014;45(8):687-97.DOI: 10.1016/j.arcmed.2014.11.013.
41. Oby E, Janigro D. The blood-brain barrier and epilepsy. Epilepsia. 2006;47(11):1761-74.DOI: 10.1111/j.1528-1167.2006.00817.x.
42. Alexandrov PN, Hill JM, Zhao Y, Bond T, Taylor CM, Percy ME, Li W, Lukiw WJ. Aluminum-induced generation of lipopolysaccharide (LPS) from the human gastrointestinal (GI)-tract microbiome-resident Bacteroides fragilis. J Inorg Biochem. 2020;203:110886.DOI: 10.1016/j.jinorgbio.2019.110886.

43. Abbott NJ, Friedman A. Overview and introduction: The blood–brain barrier in health and disease. Epilepsia. 2012;53(s6):1-6.DOI: https://doi.org/10.1111/j.1528-1167.2012.03696.x.
44. Zou P, Yang F, Ding Y, Zhang D, Liu Y, Zhang J, Wu D, Wang Y. Lipopolysaccharide downregulates the expression of ZO-1 protein through the Akt pathway. BMC Infectious Diseases. 2022;22(1):774.DOI: 10.1186/s12879-022-07752-1.
45. Hartz AM, Bauer B, Fricker G, Miller DS. Rapid modulation of P-glycoprotein-mediated transport at the blood-brain barrier by tumor necrosis factor-alpha and lipopolysaccharide. Molecular pharmacology. 2006;69(2):462-70.DOI: 10.1124/mol.105.017954.
46. Bauer B, Hartz AM, Miller DS. Tumor necrosis factor alpha and endothelin-1 increase P-glycoprotein expression and transport activity at the blood-brain barrier. Molecular pharmacology. 2007;71(3):667-75.DOI: 10.1124/mol.106.029512.
47. von Wedel-Parlow M, Wölte P, Galla HJ. Regulation of major efflux transporters under inflammatory conditions at the blood-brain barrier in vitro. Journal of neurochemistry. 2009;111(1):111-8.DOI: 10.1111/j.1471-4159.2009.06305.x.
48. Simon MJ, Iliff JJ. Regulation of cerebrospinal fluid (CSF) flow in neurodegenerative, neurovascular and neuroinflammatory disease. Biochim Biophys Acta. 2016;1862(3):442-51.DOI: 10.1016/j.bbadis.2015.10.014.
49. Mogensen FL, Delle C, Nedergaard M. The Glymphatic System (En)during Inflammation. Int J Mol Sci. 2021;22(14).DOI: 10.3390/ijms22147491.
50. Erickson MA, Hartvigson PE, Morofuji Y, Owen JB, Butterfield DA, Banks WA. Lipopolysaccharide impairs amyloid β efflux from brain: altered vascular sequestration, cerebrospinal fluid reabsorption, peripheral clearance and transporter function at the blood-brain barrier. Journal of neuroinflammation. 2012;9:150.DOI: 10.1186/1742-2094-9-150.
51. Tunblad K, Ederoth P, Gardenfors A, Hammarlund-Udenaes M, Nordstrom CH. Altered brain exposure of morphine in experimental meningitis studied with microdialysis. Acta anaesthesiologica Scandinavica. 2004;48(3):294-301.DOI: 10.1111/j.0001-5172.2003.0311.x.
52. Ederoth P, Tunblad K, Bouw R, Lundberg CJ, Ungerstedt U, Nordström CH, Hammarlund-Udenaes M. Blood-brain barrier transport of morphine in patients with severe brain trauma. British journal of clinical pharmacology. 2004;57(4):427-35.DOI: 10.1046/j.1365-2125.2003.02032.x.
53. Kawase A, Kazaoka A, Shimada H, Iwaki M. Increased brain penetration of diphenhydramine and memantine in rats with adjuvant-induced arthritis. Brain research. 2021;1768:147581.DOI: 10.1016/j.brainres.2021.147581.
54. Kawase A, Chuma T, Irie K, Kazaoka A, Kakuno A, Matsuda N, Shimada H, Iwaki M. Increased penetration of diphenhydramine in brain via proton-coupled organic cation antiporter in rats with lipopolysaccharide-induced inflammation. Brain Behavior and Immunity - Health. 2021;10:100188.DOI: https://doi.org/10.1016/j.bbih.2020.100188.
55. Sanchez-Covarrubias L, Slosky LM, Thompson BJ, Davis TP, Ronaldson PT. Transporters at CNS barrier sites: obstacles or opportunities for drug delivery? Current pharmaceutical design. 2014;20(10):1422-49.
DOI: 10.2174/13816128113199990463.
56. Puris E, Fricker G, Gynther M. Targeting Transporters for Drug Delivery to the Brain: Can We Do Better? Pharmaceutical research. 2022.
DOI: 10.1007/s11095-022-03241-x.

57. Pardridge WM. Drug transport across the blood-brain barrier. Journal of cerebral blood flow and metabolism : official journal of the International Society of Cerebral Blood Flow and Metabolism. 2012;32(11):1959-72.DOI: 10.1038/jcbfm.2012.126.
58. Kageyama T, Nakamura M, Matsuo A, Yamasaki Y, Takakura Y, Hashida M, Kanai Y, Naito M, Tsuruo T, Minato N, Shimohama S. The 4F2hc/LAT1 complex transports L-DOPA across the blood-brain barrier. Brain research. 2000;879(1-2):115-21.DOI: 10.1016/s0006-8993(00)02758-x.
59. Goldberg MJ, Spector R, Chiang CK. Transport of diphenhydramine in the central nervous system. Journal of Pharmacology and Experimental Therapeutics. 1987;240(3):717-22.DOI.
60. Yamazaki M, Fukuoka H, Nagata O, Kato H, Ito Y, Terasaki T, Tsuji A. Transport mechanism of an H1-antagonist at the blood-brain barrier: transport mechanism of mepyramine using the carotid injection technique. Biological & pharmaceutical bulletin. 1994;17(5):676-9.DOI: 10.1248/bpb.17.676.
61. Yamazaki M, Terasaki T, Yoshioka K, Nagata O, Kato H, Ito Y, Tsuji A. Carrier-mediated transport of H1-antagonist at the blood-brain barrier: mepyramine uptake into bovine brain capillary endothelial cells in primary monolayer cultures. Pharmaceutical research. 1994;11(7):975-8.
DOI: 10.1023/a:1018923017954.
62. Sachkova A, Jensen O, Dücker C, Ansari S, Brockmöller J. The mystery of the human proton-organic cation antiporter: One transport protein or many? Pharmacol Ther. 2022;239:108283.DOI: 10.1016/j.pharmthera.2022.108283.
63. Boström E, Simonsson US, Hammarlund-Udenaes M. In vivo blood-brain barrier transport of oxycodone in the rat: indications for active influx and implications for pharmacokinetics/pharmacodynamics. Drug metabolism and disposition: the biological fate of chemicals. 2006;34(9):1624-31.DOI: 10.1124/dmd.106.009746.
64. Okura T, Hattori A, Takano Y, Sato T, Hammarlund-Udenaes M, Terasaki T, Deguchi Y. Involvement of the pyrilamine transporter, a putative organic cation transporter, in blood-brain barrier transport of oxycodone. Drug metabolism and disposition: the biological fate of chemicals. 2008;36(10):2005-13.DOI: 10.1124/dmd.108.022087.
65. Shimomura K, Okura T, Kato S, Couraud PO, Schermann JM, Terasaki T, Deguchi Y. Functional expression of a proton-coupled organic cation (H+/OC) antiporter in human brain capillary endothelial cell line hCMEC/D3, a human blood-brain barrier model. Fluids and barriers of the CNS. 2013;10(1):8.DOI: 10.1186/2045-8118-10-8.
66. Kitamura A, Okura T, Higuchi K, Deguchi Y. Cocktail-Dosing Microdialysis Study to Simultaneously Assess Delivery of Multiple Organic-Cationic Drugs to the Brain. Journal of pharmaceutical sciences. 2016;105(2):935-40.DOI: 10.1002/jps.24691.
67. Chaves C, Remiao F, Cisternino S, Decleves X. Opioids and the Blood-Brain Barrier: A Dynamic Interaction with Consequences on Drug Disposition in Brain. Current neuropharmacology. 2017;15(8):1156-73.DOI: 10.2174/1570159x15666170504095823.
68. Sadiq MW, Borgs A, Okura T, Shimomura K, Kato S, Deguchi Y, Jansson B, Bjorkman S, Terasaki T, Hammarlund-Udenaes M. Diphenhydramine active uptake at the blood-brain barrier and its interaction with oxycodone in vitro and in vivo. Journal of pharmaceutical sciences. 2011;100(9):3912-23.DOI: 10.1002/jps.22567.

69. Kurosawa T, Higuchi K, Okura T, Kobayashi K, Kusuhara H, Deguchi Y. Involvement of Proton-Coupled Organic Cation Antiporter in Varenicline Transport at Blood-Brain Barrier of Rats and in Human Brain Capillary Endothelial Cells. Journal of pharmaceutical sciences. 2017;106(9):2576-82.DOI: 10.1016/j.xphs.2017.04.032.
70. Kitamura A, Higuchi K, Okura T, Deguchi Y. Transport characteristics of tramadol in the blood-brain barrier. Journal of pharmaceutical sciences. 2014;103(10):3335-41.DOI: 10.1002/jps.24129.
71. Doetsch DA, Ansari S, Jensen O, Gebauer L, Dücker C, Brockmöller J, Sachkova A. Substrates of the Human Brain Proton-Organic Cation Antiporter and Comparison with Organic Cation Transporter 1 Activities. Int J Mol Sci. 2022;23(15).DOI: 10.3390/ijms23158430.
72. Hesselink MB, De Boer BG, Breimer DD, Danysz W. Brain penetration and in vivo recovery of NMDA receptor antagonists amantadine and memantine: a quantitative microdialysis study. Pharm Res. 1999;16(5):637-42.DOI: 10.1023/a:1018856020583.
73. Higuchi K, Kitamura A, Okura T, Deguchi Y. Memantine transport by a proton-coupled organic cation antiporter in hCMEC/D3 cells, an in vitro human blood-brain barrier model. Drug Metab Pharmacokinet. 2015;30(2):182-7.DOI: 10.1016/j.dmpk.2014.12.006.
74. Mehta DC, Short JL, Nicolazzo JA. Memantine transport across the mouse blood-brain barrier is mediated by a cationic influx H+ antiporter. Molecular pharmaceutics. 2013;10(12):4491-8.DOI: 10.1021/mp400316e.
75. Fridén M, Bergström F, Wan H, Rehngren M, Ahlin G, Hammarlund-Udenaes M, Bredberg U. Measurement of unbound drug exposure in brain: modeling of pH partitioning explains diverging results between the brain slice and brain homogenate methods. Drug metabolism and disposition: the biological fate of chemicals. 2011;39(3):353-62.DOI: 10.1124/dmd.110.035998.
76. De Duve C, De Barsy T, Poole B, Trouet A, Tulkens P, Van Hoof Fo. Lysosomotropic agents. Biochemical pharmacology. 1974;23(18):2495-531.DOI: https://doi.org/10.1016/0006-2952(74)90174-9.
77. Smirnova M, Goracci L, Cruciani G, Federici L, Declèves X, Chapy H, Cisternino S. Pharmacophore-Based Discovery of Substrates of a Novel Drug/Proton-Antiporter in the Human Brain Endothelial hCMEC/D3 Cell Line. Pharmaceutics. 2022;14(2).DOI: 10.3390/pharmaceutics14020255.
78. Kurosawa T, Tega Y, Uchida Y, Higuchi K, Tabata H, Sumiyoshi T, Kubo Y, Terasaki T, Deguchi Y. Proteomics-Based Transporter Identification by the PICK Method: Involvement of TM7SF3 and LHFPL6 in Proton-Coupled Organic Cation Antiport at the Blood-Brain Barrier. Pharmaceutics. 2022;14(8).DOI: 10.3390/pharmaceutics14081683.
79. Fridén M, Winiwarter S, Jerndal G, Bengtsson O, Wan H, Bredberg U, Hammarlund-Udenaes M, Antonsson M. Structure-brain exposure relationships in rat and human using a novel data set of unbound drug concentrations in brain interstitial and cerebrospinal fluids. Journal of medicinal chemistry. 2009;52(20):6233-43.DOI: 10.1021/jm901036q.
80. Shen DD, Artru AA, Adkison KK. Principles and applicability of CSF sampling for the assessment of CNS drug delivery and pharmacodynamics. Advanced drug delivery reviews. 2004;56(12):1825-57.DOI: 10.1016/j.addr.2004.07.011.
81. Beery AK. Inclusion of females does not increase variability in rodent research studies. Current Opinion in Behavioral Sciences. 2018;23:143-9.DOI: https://doi.org/10.1016/j.cobeha.2018.06.016.

82. Bierer BE, Meloney LG, Ahmed HR, White SA. Advancing the inclusion of underrepresented women in clinical research. Cell Rep Med. 2022;3(4):100553.DOI: 10.1016/j.xcrm.2022.100553.
83. Kaiko RF, Benziger DP, Fitzmartin RD, Burke BE, Reder RF, Goldenheim PD. Pharmacokinetic-pharmacodynamic relationships of controlled-release oxycodone. Clinical pharmacology and therapeutics. 1996;59(1):52-61.DOI: 10.1016/s0009-9236(96)90024-7.
84. Chan S, Edwards SR, Wyse BD, Smith MT. Sex differences in the pharmacokinetics, oxidative metabolism and oral bioavailability of oxycodone in the Sprague-Dawley rat. Clinical and experimental pharmacology & physiology. 2008;35(3):295-302.DOI: 10.1111/j.1440-1681.2007.04821.x.
85. Arguelles N, Miksys S, Tyndale RF. Sex and Estrous Cycle Differences in Analgesia and Brain Oxycodone Levels. Molecular neurobiology. 2021.DOI: 10.1007/s12035-021-02560-1.
86. Syvänen S, Lindhe O, Palner M, Kornum BR, Rahman O, Långström B, Knudsen GM, Hammarlund-Udenaes M. Species differences in blood-brain barrier transport of three positron emission tomography radioligands with emphasis on P-glycoprotein transport. Drug metabolism and disposition: the biological fate of chemicals. 2009;37(3):635-43.DOI: 10.1124/dmd.108.024745.
87. Kido Y, Nanchi I, Fusamae Y, Matsuzaki T, Akazawa T, Sawada H, Iwasaki M, Nishida K, Tsuchiya E, Okuda T. Species difference in brain penetration of P-gp and BCRP substrates among monkey, dog and mouse. Drug Metabolism and Pharmacokinetics. 2022;42:100426.DOI: https://doi.org/10.1016/j.dmpk.2021.100426.
88. Shaffer CL, Osgood, S.M., Mancuso, J.Y., Doran A.C. Diphenhydramine has Similar Interspecies Net Active Influx at the Blood–Brain Barrier. Journal of pharmaceutical sciences. 2014.DOI.
89. Langthaler K, Jones CR, Brodin B, Bundgaard C. Assessing extent of brain penetration in vivo (Kp,uu,brain) in Göttingen minipig using a diverse set of reference drugs. European Journal of Pharmaceutical Sciences. 2023;190:106554.DOI: https://doi.org/10.1016/j.ejps.2023.106554.
90. O'Brown NM, Pfau SJ, Gu C. Bridging barriers: a comparative look at the blood-brain barrier across organisms. Genes Dev. 2018;32(7-8):466-78.DOI: 10.1101/gad.309823.117.
91. Authier S, Arezzo J, Delatte MS, Kallman MJ, Markgraf C, Paquette D, Pugsley MK, Ratcliffe S, Redfern WS, Stevens J, Valentin JP, Vargas HM, Curtis MJ. Safety pharmacology investigations on the nervous system: An industry survey. J Pharmacol Toxicol Methods. 2016;81:37-46.DOI: 10.1016/j.vascn.2016.06.001.
92. Cook D, Brown D, Alexander R, March R, Morgan P, Satterthwaite G, Pangalos MN. Lessons learned from the fate of AstraZeneca's drug pipeline: a five-dimensional framework. Nature Reviews Drug Discovery. 2014;13(6):419-31.DOI: 10.1038/nrd4309.
93. Edwards IR, Aronson JK. Adverse drug reactions: definitions, diagnosis, and management. Lancet. 2000;356(9237):1255-9.DOI: 10.1016/s0140-6736(00)02799-9.
94. Andronis C, Silva JP, Lekka E, Virvilis V, Carmo H, Bampali K, Ernst M, Hu Y, Loryan I, Richard J, Carvalho F, Savić MM. Molecular basis of mood and cognitive adverse events elucidated via a combination of pharmacovigilance data mining and functional enrichment analysis. Archives of toxicology. 2020;94(8):2829-45.DOI: 10.1007/s00204-020-02788-1.

95. Lipponen A, Kajevu N, Natunen T, Ciszek R, Puhakka N, Hiltunen M, Pitkänen A. Gene Expression Profile as a Predictor of Seizure Liability. International Journal of Molecular Sciences. 2023;24(4):4116.DOI: https://doi.org/10.3390/ijms24044116.
96. Cremers TI, Flik G, Folgering JH, Rollema H, Stratford RE, Jr. Development of a Rat Plasma and Brain Extracellular Fluid Pharmacokinetic Model for Bupropion and Hydroxybupropion Based on Microdialysis Sampling, and Application to Predict Human Brain Concentrations. Drug metabolism and disposition: the biological fate of chemicals. 2016;44(5):624-33.DOI: 10.1124/dmd.115.068932.
97. Zhai J, Traebert M, Zimmermann K, Delaunois A, Royer L, Salvagiotto G, Carlson C, Lagrutta A. Comparative study for the IMI2-NeuroDeRisk project on microelectrode arrays to derisk drug-induced seizure liability. Journal of Pharmacological and Toxicological Methods. 2023;123:107297.DOI: https://doi.org/10.1016/j.vascn.2023.107297.
98. Cavarec L, Vincent L, Le Borgne C, Plusquellec C, Ollivier N, Normandie-Levi P, Allemand F, Salvetat N, Mathieu-Dupas E, Molina F, Weissmann D, Pujol J-F. In Vitro Screening for Drug-Induced Depression and/or Suicidal Adverse Effects: A New Toxicogenomic Assay Based on CE-SSCP Analysis of HTR2C mRNA Editing in SH-SY5Y Cells. Neurotoxicity Research. 2013;23(1):49-62.DOI: 10.1007/s12640-012-9324-9.
99. Hammarlund-Udenaes M, Fridén M, Syvanen S, Gupta A. On the rate and extent of drug delivery to the brain. Pharmaceutical research. 2008;25(8):1737-50.DOI: 10.1007/s11095-007-9502-2.
100. Smith DA, Di L, Kerns EH. The effect of plasma protein binding on in vivo efficacy: misconceptions in drug discovery. Nature reviews Drug discovery. 2010;9(12):929-39.DOI: 10.1038/nrd3287.
101. Summerfield SG, Yates JWT, Fairman DA. Free Drug Theory – No Longer Just a Hypothesis? Pharmaceutical research. 2022;39(2):213-22.DOI: 10.1007/s11095-022-03172-7.
102. Gupta A, Chatelain P, Massingham R, Jonsson EN, Hammarlund-Udenaes M. Brain distribution of cetirizine enantiomers: comparison of three different tissue-to-plasma partition coefficients: K(p), K(p,u), and K(p,uu). Drug metabolism and disposition: the biological fate of chemicals. 2006;34(2):318-23.DOI: 10.1124/dmd.105.007211.
103. Hammarlund-Udenaes M, Paalzow LK, de Lange EC. Drug equilibration across the blood-brain barrier--pharmacokinetic considerations based on the microdialysis method. Pharmaceutical research. 1997;14(2):128-34.DOI: 10.1023/a:1012080106490.
104. Loryan I, Reichel A, Feng B, Bundgaard C, Shaffer C, Kalvass C, Bednarczyk D, Morrison D, Lesuisse D, Hoppe E, Terstappen GC, Fischer H, Di L, Colclough N, Summerfield S, Buckley ST, Maurer TS, Fridén M. Unbound Brain-to-Plasma Partition Coefficient, K(p,uu,brain)-a Game Changing Parameter for CNS Drug Discovery and Development. Pharm Res. 2022;39(7):1321-41.DOI: 10.1007/s11095-022-03246-6.
105. Loryan I, Sinha V, Mackie C, Van Peer A, Drinkenburg W, Vermeulen A, Morrison D, Monshouwer M, Heald D, Hammarlund-Udenaes M. Mechanistic understanding of brain drug disposition to optimize the selection of potential neurotherapeutics in drug discovery. Pharm Res. 2014;31(8):2203-19.DOI: 10.1007/s11095-014-1319-1.

106. Wang W. The Simultaneous Estimation Of The Influx and Efflux Blood-Brain Barrier Permeabilities of Gabapentin Using a Microdialysis Pharmacokinetic Approach. 1996.DOI.
107. Hammarlund-Udenaes M. Microdialysis in CNS PKPD Research: Unraveling Unbound Concentrations. In: Müller M, editor. Microdialysis in Drug Development. New York, NY: Springer New York; 2013. p. 83-102.
108. Fridén M, Ducrozet F, Middleton B, Antonsson M, Bredberg U, Hammarlund-Udenaes M. Development of a high-throughput brain slice method for studying drug distribution in the central nervous system. Drug metabolism and disposition: the biological fate of chemicals. 2009;37(6):1226-33.DOI: 10.1124/dmd.108.026377.
109. Loryan I, Fridén M, Hammarlund-Udenaes M. The brain slice method for studying drug distribution in the CNS. Fluids and barriers of the CNS. 2013;10(1):6.DOI: 10.1186/2045-8118-10-6.
110. Kalvass JC, Maurer TS. Influence of nonspecific brain and plasma binding on CNS exposure: implications for rational drug discovery. Biopharmaceutics & drug disposition. 2002;23(8):327-38.DOI: 10.1002/bdd.325.
111. Wan H, Rehngren M, Giordanetto F, Bergstrom F, Tunek A. High-throughput screening of drug-brain tissue binding and in silico prediction for assessment of central nervous system drug delivery. Journal of medicinal chemistry. 2007;50(19):4606-15.DOI: 10.1021/jm070375w.
112. Hammarlund-Udenaes M. Microdialysis as an Important Technique in Systems Pharmacology-a Historical and Methodological Review. Aaps j. 2017;19(5):1294-303.DOI: 10.1208/s12248-017-0108-2.
113. Nelson DW, Thornquist B, MacCallum RM, Nyström H, Holst A, Rudehill A, Wanecek M, Bellander B-M, Weitzberg E. Analyses of cerebral microdialysis in patients with traumatic brain injury: relations to intracranial pressure, cerebral perfusion pressure and catheter placement. BMC Medicine. 2011;9(1):21.DOI: 10.1186/1741-7015-9-21.
114. de Lange EC. Utility of CSF in translational neuroscience. Journal of pharmacokinetics and pharmacodynamics. 2013;40(3):315-26.DOI: 10.1007/s10928-013-9301-9.
115. MacAulay N, Keep RF, Zeuthen T. Cerebrospinal fluid production by the choroid plexus: a century of barrier research revisited. Fluids and barriers of the CNS. 2022;19(1):26-.DOI: 10.1186/s12987-022-00323-1.
116. Hladky SB, Barrand MA. Mechanisms of fluid movement into, through and out of the brain: evaluation of the evidence. Fluids and barriers of the CNS. 2014;11(1):26.DOI: 10.1186/2045-8118-11-26.
117. Saleh MAA, Loo CF, Elassaiss-Schaap J, De Lange ECM. Lumbar cerebrospinal fluid-to-brain extracellular fluid surrogacy is context-specific: insights from LeiCNS-PK3.0 simulations. Journal of pharmacokinetics and pharmacodynamics. 2021.DOI: 10.1007/s10928-021-09768-7.
118. Srinivas N, Maffuid K, Kashuba ADM. Clinical Pharmacokinetics and Pharmacodynamics of Drugs in the Central Nervous System. Clinical pharmacokinetics. 2018;57(9):1059-74.DOI: 10.1007/s40262-018-0632-y.
119. Liu X, Van Natta K, Yeo H, Vilenski O, Weller PE, Worboys PD, Monshouwer M. Unbound Drug Concentration in Brain Homogenate and Cerebral Spinal Fluid at Steady State as a Surrogate for Unbound Concentration in Brain Interstitial Fluid. Drug Metabolism and Disposition. 2009;37(4):787-93.DOI: 10.1124/dmd.108.024125.

120. Saleh MAA, Bloemberg JS, Elassaiss-Schaap J, de Lange ECM. Drug Distribution in Brain and Cerebrospinal Fluids in Relation to IC(50) Values in Aging and Alzheimer's Disease, Using the Physiologically Based LeiCNS-PK3.0 Model. Pharmaceutical research. 2022;39(7):1303-19.DOI: 10.1007/s11095-022-03281-3.
121. Friden M, Winiwarter S, Jerndal G, Bengtsson O, Wan H, Bredberg U, Hammarlund-Udenaes M, Antonsson M. Structure-brain exposure relationships in rat and human using a novel data set of unbound drug concentrations in brain interstitial and cerebrospinal fluids. Journal of medicinal chemistry. 2009;52(20):6233-43.DOI: 10.1021/jm901036q.
122. Fridén M, Gupta A, Antonsson M, Bredberg U, Hammarlund-Udenaes M. In vitro methods for estimating unbound drug concentrations in the brain interstitial and intracellular fluids. Drug metabolism and disposition: the biological fate of chemicals. 2007;35(9):1711-9.DOI: 10.1124/dmd.107.015222.
123. Luptáková D, Vallianatou T, Nilsson A, Shariatgorji R, Hammarlund-Udenaes M, Loryan I, Andrén PE. Neuropharmacokinetic visualization of regional and subregional unbound antipsychotic drug transport across the blood-brain barrier. Molecular psychiatry. 2021.DOI: 10.1038/s41380-021-01267-y.
124. Helms HC, Abbott NJ, Burek M, Cecchelli R, Couraud PO, Deli MA, Forster C, Galla HJ, Romero IA, Shusta EV, Stebbins MJ, Vandenhaute E, Weksler B, Brodin B. In vitro models of the blood-brain barrier: An overview of commonly used brain endothelial cell culture models and guidelines for their use. Journal of cerebral blood flow and metabolism : official journal of the International Society of Cerebral Blood Flow and Metabolism. 2016;36(5):862-90.DOI: 10.1177/0271678x16630991.
125. Weksler BB, Subileau EA, Perriere N, Charneau P, Holloway K, Leveque M, Tricoire-Leignel H, Nicotra A, Bourdoulous S, Turowski P, Male DK, Roux F, Greenwood J, Romero IA, Couraud PO. Blood-brain barrier-specific properties of a human adult brain endothelial cell line. FASEB journal : official publication of the Federation of American Societies for Experimental Biology. 2005;19(13):1872-4.DOI: 10.1096/fj.04-3458fje.
126. Weksler B, Romero IA, Couraud P-O. The hCMEC/D3 cell line as a model of the human blood brain barrier. Fluids and barriers of the CNS. 2013;10(1):16.DOI: 10.1186/2045-8118-10-16.
127. Svane N, Pedersen ABV, Rodenberg A, Ozgür B, Saaby L, Bundgaard C, Kristensen M, Tfelt-Hansen P, Brodin B. The putative proton-coupled organic cation antiporter is involved in uptake of triptans into human brain capillary endothelial cells. Fluids and barriers of the CNS. 2024;21(1):39.DOI: 10.1186/s12987-024-00544-6.
128. Urich E, Lazic SE, Molnos J, Wells I, Freskgård PO. Transcriptional profiling of human brain endothelial cells reveals key properties crucial for predictive in vitro blood-brain barrier models. PloS one. 2012;7(5):e38149.DOI: 10.1371/journal.pone.0038149.
129. Veszelka S, Tóth A, Walter FR, Tóth AE, Gróf I, Mészáros M, Bocsik A, Hellinger É, Vastag M, Rákhely G, Deli MA. Comparison of a Rat Primary Cell-Based Blood-Brain Barrier Model With Epithelial and Brain Endothelial Cell Lines: Gene Expression and Drug Transport. Frontiers in Molecular Neuroscience. 2018;11.DOI: 10.3389/fnmol.2018.00166.
130. Deli MA, Ábrahám CS, Kataoka Y, Niwa M. Permeability Studies on In Vitro Blood–Brain Barrier Models:Physiology, Pathology, and Pharmacology. Cellular and molecular neurobiology. 2005;25(1):59-127.DOI: 10.1007/s10571-004-1377-8.

131. Yamazaki M, Terasaki T, Yoshioka K, Nagata O, Kato H, Ito Y, Tsuji A. Carrier-Mediated Transport of H1-Antagonist at the Blood-Brain Barrier: A Common Transport System of H1-Antagonists and Lipophilic Basic Drugs. Pharmaceutical research. 1994;11(11):1516-8.DOI: 10.1023/A:1018980914687.
132. Shamul JG, Wang Z, Gong H, Ou W, White AM, Moniz-Garcia DP, Gu S, Clyne AM, Quiñones-Hinojosa A, He X. Meta-analysis of the make-up and properties of in vitro models of the healthy and diseased blood–brain barrier. Nature Biomedical Engineering. 2024.DOI: 10.1038/s41551-024-01250-2.
133. Feng B, West M, Patel NC, Wager T, Hou X, Johnson J, Tremaine L, Liras J. Validation of Human MDR1-MDCK and BCRP-MDCK Cell Lines to Improve the Prediction of Brain Penetration. Journal of pharmaceutical sciences. 2019;108(7):2476-83.DOI: 10.1016/j.xphs.2019.02.005.
134. Batista CRA, Gomes GF, Candelario-Jalil E, Fiebich BL, de Oliveira ACP. Lipopolysaccharide-Induced Neuroinflammation as a Bridge to Understand Neurodegeneration. Int J Mol Sci. 2019;20(9).DOI: 10.3390/ijms20092293.
135. Hawiger J. Innate immunity and inflammation: a transcriptional paradigm. Immunol Res. 2001;23(2-3):99-109.DOI: 10.1385/ir:23:2-3:099.
136. Gustot T. Multiple organ failure in sepsis: prognosis and role of systemic inflammatory response. Curr Opin Crit Care. 2011;17(2):153-9.DOI: 10.1097/MCC.0b013e328344b446.
137. Kellum JA, Ronco C. The role of endotoxin in septic shock. Critical Care. 2023;27(1):400.DOI: 10.1186/s13054-023-04690-5.
138. Jarczak D, Kluge S, Nierhaus A. Sepsis—Pathophysiology and Therapeutic Concepts. Frontiers in Medicine. 2021;8.DOI: 10.3389/fmed.2021.628302.
139. Wyns H, Plessers E, De Backer P, Meyer E, Croubels S. In vivo porcine lipopolysaccharide inflammation models to study immunomodulation of drugs. Veterinary immunology and immunopathology. 2015;166(3-4):58-69.DOI: 10.1016/j.vetimm.2015.06.001.
140. Andersson PB, Perry VH, Gordon S. The acute inflammatory response to lipopolysaccharide in CNS parenchyma differs from that in other body tissues. Neuroscience. 1992;48(1):169-86.DOI: 10.1016/0306-4522(92)90347-5.
141. Varatharaj A, Galea I. The blood-brain barrier in systemic inflammation. Brain, behavior, and immunity. 2017;60:1-12.DOI: 10.1016/j.bbi.2016.03.010.
142. Erickson MA, Hansen K, Banks WA. Inflammation-induced dysfunction of the low-density lipoprotein receptor-related protein-1 at the blood-brain barrier: protection by the antioxidant N-acetylcysteine. Brain, behavior, and immunity. 2012;26(7):1085-94.DOI: 10.1016/j.bbi.2012.07.003.
143. Jaeger LB, Dohgu S, Sultana R, Lynch JL, Owen JB, Erickson MA, Shah GN, Price TO, Fleegal-Demotta MA, Butterfield DA, Banks WA. Lipopolysaccharide alters the blood-brain barrier transport of amyloid beta protein: a mechanism for inflammation in the progression of Alzheimer's disease. Brain, behavior, and immunity. 2009;23(4):507-17.DOI: 10.1016/j.bbi.2009.01.017.
144. Nazem A, Sankowski R, Bacher M, Al-Abed Y. Rodent models of neuroinflammation for Alzheimer's disease. Journal of neuroinflammation. 2015;12:74.DOI: 10.1186/s12974-015-0291-y.
145. Gustafsson S, Lindström V, Ingelsson M, Hammarlund-Udenaes M, Syvänen S. Intact blood-brain barrier transport of small molecular drugs in animal models of amyloid beta and alpha-synuclein pathology. Neuropharmacology. 2018;128:482-91.DOI: 10.1016/j.neuropharm.2017.08.002.

146. Mihajlica N, Betsholtz C, Hammarlund-Udenaes M. Rate of small-molecular drug transport across the blood-brain barrier in a pericyte-deficient state. European journal of pharmaceutical sciences : official journal of the European Federation for Pharmaceutical Sciences. 2018;124:182-7.DOI: 10.1016/j.ejps.2018.08.009.
147. Mihajlica N, Betsholtz C, Hammarlund-Udenaes M. Pharmacokinetics of pericyte involvement in small-molecular drug transport across the blood-brain barrier. European journal of pharmaceutical sciences : official journal of the European Federation for Pharmaceutical Sciences. 2018;122:77-84.DOI: 10.1016/j.ejps.2018.06.018.
148. Ohshima S, Saeki Y, Mima T, Sasai M, Nishioka K, Nomura S, Kopf M, Katada Y, Tanaka T, Suemura M, Kishimoto T. Interleukin 6 plays a key role in the development of antigen-induced arthritis. Proc Natl Acad Sci U S A. 1998;95(14):8222-6.DOI: 10.1073/pnas.95.14.8222.
149. Lipcsey M, Larsson A, Olovsson M, Sjölin J, Eriksson MB. Early endotoxin-mediated haemostatic and inflammatory responses in the clopidogrel-treated pig. Platelets. 2005;16(7):408-14.DOI: 10.1080/09537100500163168.
150. Gabay C. Interleukin-6 and chronic inflammation. Arthritis Research & Therapy. 2006;8(2):S3.DOI: 10.1186/ar1917.
151. de Vries HE, Blom-Roosemalen MC, van Oosten M, de Boer AG, van Berkel TJ, Breimer DD, Kuiper J. The influence of cytokines on the integrity of the blood-brain barrier in vitro. Journal of neuroimmunology. 1996;64(1):37-43.DOI: 10.1016/0165-5728(95)00148-4.
152. Kim H, Wang I-N, Park J-S, Kim K-T, Kong J, Kim JB, Kim D-J. Inherent seizure susceptibility in patients with antihistamine-induced acute symptomatic seizure: a resting-state EEG analysis. Scientific reports. 2023;13(1):9146.DOI: 10.1038/s41598-023-36415-7.
153. Kamei C, Ohuchi M, Sugimoto Y, Okuma C. Mechanism responsible for epileptogenic activity by first-generation H1-antagonists in rats. Brain research. 2000;887(1):183-6.DOI: https://doi.org/10.1016/S0006-8993(00)03041-9.
154. Klein M, Rudich Z, Gurevich B, Lifshitz M, Brill S, Lottan M, Weksler N. Controlled-release oxycodone-induced seizures. Clinical Therapeutics. 2005;27(11):1815-8.DOI: https://doi.org/10.1016/j.clinthera.2005.11.001.
155. Krzywinski M, Altman N. Power and sample size. Nature Methods. 2013;10(12):1139-40.DOI: 10.1038/nmeth.2738.
156. Paxinos G, Watson C. In: Paxinos G, Watson C, editors. The Rat Brain (Second Edition): Academic Press; 1986. p. iv.
157. Bouw MR, Hammarlund-Udenaes M. Methodological aspects of the use of a calibrator in in vivo microdialysis-further development of the retrodialysis method. Pharmaceutical research. 1998;15(11):1673-9.DOI: 10.1023/a:1011992125204.
158. Strandberg G, Larsson A, Lipcsey M, Berglund L, Eriksson M. Analysis of intraosseous samples in endotoxemic shock--an experimental study in the anaesthetised pig. Acta anaesthesiologica Scandinavica. 2014;58(3):337-44.DOI: 10.1111/aas.12274.
159. Lipcsey M, Larsson A, Eriksson MB, Sjölin J. Inflammatory, coagulatory and circulatory responses to logarithmic increases in the endotoxin dose in the anaesthetised pig. J Endotoxin Res. 2006;12(2):99-112.DOI: 10.1179/096805106x89053.
160. Lipcsey M, Larsson A, Eriksson MB, Sjölin J. Effect of the administration rate on the biological responses to a fixed dose of endotoxin in the anesthetized pig. Shock. 2008;29(2):173-80.DOI: 10.1097/SHK.0b013e318067dfbc.

161. Rutai A, Zsikai B, Tallósy SP, Érces D, Bizánc L, Juhász L, Poles MZ, Sóki J, Baaity Z, Fejes R, Varga G, Földesi I, Burián K, Szabó A, Boros M, Kaszaki J. A Porcine Sepsis Model With Numerical Scoring for Early Prediction of Severity. Front Med (Lausanne). 2022;9:867796.DOI: 10.3389/fmed.2022.867796.
162. Hu Y, Girdenyté M, Roest L, Liukkonen I, Siskou M, Bällgren F, Hammarlund-Udenaes M, Loryan I. Analysis of the contributing role of drug transport across biological barriers in the development and treatment of chemotherapy-induced peripheral neuropathy. Fluids and barriers of the CNS. 2024;21(1):13.DOI: 10.1186/s12987-024-00519-7.
163. Gustafsson S, Gustavsson T, Roshanbin S, Hultqvist G, Hammarlund-Udenaes M, Sehlin D, Syvänen S. Blood-brain barrier integrity in a mouse model of Alzheimer's disease with or without acute 3D6 immunotherapy. Neuropharmacology. 2018;143:1-9.DOI: 10.1016/j.neuropharm.2018.09.001.
164. Loryan I, Hoppe E, Hansen K, Held F, Kless A, Linz K, Marossek V, Nolte B, Ratcliffe P, Saunders D, Terlinden R, Wegert A, Welbers A, Will O, Hammarlund-Udenaes M. Quantitative Assessment of Drug Delivery to Tissues and Association with Phospholipidosis: A Case Study with Two Structurally Related Diamines in Development. Molecular pharmaceutics. 2017;14(12):4362-73.DOI: 10.1021/acs.molpharmaceut.7b00480.
165. Mateus A, Matsson P, Artursson P. Rapid Measurement of Intracellular Unbound Drug Concentrations. Molecular pharmaceutics. 2013;10(6):2467-78.DOI: 10.1021/mp4000822.
166. Kristensen M, Kucharz K, Felipe Alves Fernandes E, Strømgaard K, Schallburg Nielsen M, Cederberg Helms HC, Bach A, Ulrikkaholm Tofte-Hansen M, Irene Aldana Garcia B, Lauritzen M, Brodin B. Conjugation of Therapeutic PSD-95 Inhibitors to the Cell-Penetrating Peptide Tat Affects Blood-Brain Barrier Adherence, Uptake, and Permeation. Pharmaceutics. 2020;12(7).DOI: 10.3390/pharmaceutics12070661.
167. Nielsen SSE, Siupka P, Georgian A, Preston JE, Tóth AE, Yusof SR, Abbott NJ, Nielsen MS. Improved Method for the Establishment of an In Vitro Blood-Brain Barrier Model Based on Porcine Brain Endothelial Cells. J Vis Exp. 2017(127).DOI: 10.3791/56277.
168. Hassan HE, Myers AL, Lee IJ, Coop A, Eddington ND. Oxycodone induces overexpression of P-glycoprotein (ABCB1) and affects paclitaxel's tissue distribution in Sprague Dawley rats. Journal of pharmaceutical sciences. 2007;96(9):2494-506.DOI: 10.1002/jps.20893.
169. Hassan HE, Myers AL, Lee IJ, Chen H, Coop A, Eddington ND. Regulation of gene expression in brain tissues of rats repeatedly treated by the highly abused opioid agonist, oxycodone: microarray profiling and gene mapping analysis. Drug metabolism and disposition: the biological fate of chemicals. 2010;38(1):157-67.DOI: 10.1124/dmd.109.029199.
170. Boström E, Simonsson US, Hammarlund-Udenaes M. Oxycodone pharmacokinetics and pharmacodynamics in the rat in the presence of the P-glycoprotein inhibitor PSC833. Journal of pharmaceutical sciences. 2005;94(5):1060-6.DOI: 10.1002/jps.20327.
171. Yabuuchi H, Tamai I, Nezu JI, Sakamoto K, Oku A, Shimane M, Sai Y, Tsuji A, editors. Novel membrane transporter OCTN1 mediates multispecific, bidirectional, and pH-dependent transport of organic cations. Journal of Pharmacology and Experimental Therapeutics; 1999.

172. Grigat S, Harlfinger S, Pal S, Striebinger R, Golz S, Geerts A, Lazar A, Schömig E, Gründemann D. Probing the substrate specificity of the ergothioneine transporter with methimazole, hercynine, and organic cations. Biochemical pharmacology. 2007;74(2):309-16.DOI: https://doi.org/10.1016/j.bcp.2007.04.015.
173. Ohashi R, Tamai I, Inano A, Katsura M, Sai Y, Nezu J-i, Tsuji A. Studies on Functional Sites of Organic Cation/Carnitine Transporter OCTN2 (SLC22A5) Using a Ser467Cys Mutant Protein. Journal of Pharmacology and Experimental Therapeutics. 2002;302(3):1286-94.DOI: 10.1124/jpet.102.036004.
174. Obradovic T, Dobson G, Shingaki T, Kungu T, Hidalgo I. Assessment of the First and Second Generation Antihistamines Brain Penetration and Role of P-Glycoprotein. Pharmaceutical research. 2007;24:318-27.DOI: 10.1007/s11095-006-9149-4.
175. Chen C, Hanson E, Watson JW, Lee JS. P-glycoprotein limits the brain penetration of nonsedating but not sedating H1-antagonists. Drug metabolism and disposition: the biological fate of chemicals. 2003;31(3):312-8.DOI: 10.1124/dmd.31.3.312.
176. Julku U, Xiong M, Wik E, Roshanbin S, Sehlin D, Syvänen S. Brain pharmacokinetics of mono- and bispecific amyloid-β antibodies in wild-type and Alzheimer's disease mice measured by high cut-off microdialysis. Fluids and barriers of the CNS. 2022;19(1):99.DOI: 10.1186/s12987-022-00398-w.
177. May LT, Santhanam U, Sehgal PB. On the multimeric nature of natural human interleukin-6. The Journal of biological chemistry. 1991;266 15:9950-5.DOI.
178. Proudfoot AE, Borlat F. Purification of recombinant chemokines from E. coli. Methods in molecular biology (Clifton, NJ). 2000;138:75-87.DOI: 10.1385/1-59259-058-6:75.
179. Banks WA, Kastin AJ, Gutierrez EG. Penetration of interleukin-6 across the murine blood-brain barrier. Neuroscience Letters. 1994;179(1):53-6.DOI: https://doi.org/10.1016/0304-3940(94)90933-4.
180. Lipcsey M, Olovsson M, Larsson E, Einarsson R, Qadhr GA, Sjölin J, Larsson A. The brain is a source of S100B increase during endotoxemia in the pig. Anesthesia and analgesia. 2010;110(1):174-80.DOI: 10.1213/ANE.0b013e3181c0724a.
181. Lipcsey M, Söderberg E, Basu S, Larsson A, Sjölin J, Aström M, Eriksson MB. F2-isoprostane, inflammation, cardiac function and oxygenation in the endotoxaemic pig. Prostaglandins Leukot Essent Fatty Acids. 2008;78(3):209-17.DOI: 10.1016/j.plefa.2008.01.006.
182. Cartmell T, Mitchell D, Lamond FJD, Laburn HP. Route of Administration Differentially Affects Fevers Induced by Gram-Negative and Gram-Positive Pyrogens in Rabbits. Experimental Physiology. 2002;87(3):391-9.DOI: https://doi.org/10.1113/eph8702298.
183. Olney KC, de Ávila C, Todd KT, Tallant LE, Barnett JH, Gibson KA, Hota P, Pandiane AS, Durgun PC, Serhan M, Wang R, Lind ML, Forzani E, Gades NM, Thomas LF, Fryer JD. Commonly disrupted pathways in brain and kidney in a pig model of systemic endotoxemia. Journal of neuroinflammation. 2024;21(1):9.DOI: 10.1186/s12974-023-03002-6.
184. De Maio A, Torres MB, Reeves RH. GENETIC DETERMINANTS INFLUENCING THE RESPONSE TO INJURY, INFLAMMATION, AND SEPSIS. Shock. 2005;23(1):11-7.DOI: 10.1097/01.shk.0000144134.03598.c5.

185. Xu Y, He Q, Wang M, Wang X, Gong F, Bai L, Zhang J, Wang W. Quantifying blood-brain-barrier leakage using a combination of evans blue and high molecular weight FITC-Dextran. Journal of neuroscience methods. 2019;325:108349.DOI: 10.1016/j.jneumeth.2019.108349.
186. Banks WA, Gray AM, Erickson MA, Salameh TS, Damodarasamy M, Sheibani N, Meabon JS, Wing EE, Morofuji Y, Cook DG, Reed MJ. Lipopolysaccharide-induced blood-brain barrier disruption: roles of cyclooxygenase, oxidative stress, neuroinflammation, and elements of the neurovascular unit. Journal of neuroinflammation. 2015;12:223.DOI: 10.1186/s12974-015-0434-1.
187. Peng X, Luo Z, He S, Zhang L, Li Y. Blood-Brain Barrier Disruption by Lipopolysaccharide and Sepsis-Associated Encephalopathy. Front Cell Infect Microbiol. 2021;11:768108.DOI: 10.3389/fcimb.2021.768108.
188. Larsson A, Lipcsey M, Sjölin J, Hansson LO, Eriksson MB. Slight increase of serum S-100B during porcine endotoxemic shock may indicate blood-brain barrier damage. Anesthesia and analgesia. 2005;101(5):1465-9.DOI: 10.1213/01.Ane.0000180193.29655.6a.
189. Salkeni MA, Lynch JL, Otamis-Price T, Banks WA. Lipopolysaccharide impairs blood-brain barrier P-glycoprotein function in mice through prostaglandin- and nitric oxide-independent pathways. J Neuroimmune Pharmacol. 2009;4(2):276-82.DOI: 10.1007/s11481-008-9138-y.
190. Torres-Vergara P, Penny J. Pro-inflammatory and anti-inflammatory compounds exert similar effects on P-glycoprotein in blood–brain barrier endothelial cells. Journal of Pharmacy and Pharmacology. 2018;70(6):713-22.DOI: 10.1111/jphp.12893.
191. Lalovic B, Phillips B, Risler LL, Howald W, Shen DD. Quantitative contribution of CYP2D6 and CYP3A to oxycodone metabolism in human liver and intestinal microsomes. Drug metabolism and disposition: the biological fate of chemicals. 2004;32(4):447-54.DOI: 10.1124/dmd.32.4.447.
192. American Society of Health-System Pharmacists A. Oxycodone (Monograph): Drugs.com; 2023 [Available from: https://www.drugs.com/monograph/oxycodone.html.
193. Grönlund J, Saari TI, Hagelberg NM, Neuvonen PJ, Olkkola KT, Laine K. Exposure to oral oxycodone is increased by concomitant inhibition of CYP2D6 and 3A4 pathways, but not by inhibition of CYP2D6 alone. British journal of clinical pharmacology. 2010;70(1):78-87.DOI: 10.1111/j.1365-2125.2010.03653.x.
194. Klöditz K, Tewolde E, Nordling Å, Ingelman-Sundberg M. Mechanistic, Functional, and Clinical Aspects of Pro-inflammatory Cytokine Mediated Regulation of ADME Gene Expression in 3D Human Liver Spheroids. Clinical pharmacology and therapeutics. 2023;114(3):673-85.DOI: 10.1002/cpt.2969.
195. Uchida Y, Yagi Y, Takao M, Tano M, Umetsu M, Hirano S, Usui T, Tachikawa M, Terasaki T. Comparison of Absolute Protein Abundances of Transporters and Receptors among Blood-Brain Barriers at Different Cerebral Regions and the Blood-Spinal Cord Barrier in Humans and Rats. Mol Pharm. 2020;17(6):2006-20.DOI: 10.1021/acs.molpharmaceut.0c00178.
196. Kubo Y, Ohtsuki S, Uchida Y, Terasaki T. Quantitative Determination of Luminal and Abluminal Membrane Distributions of Transporters in Porcine Brain Capillaries by Plasma Membrane Fractionation and Quantitative Targeted Proteomics. Journal of pharmaceutical sciences. 2015;104(9):3060-8.DOI: https://doi.org/10.1002/jps.24398.

197. Pöyhiä R, Seppälä T, Olkkola KT, Kalso E. The pharmacokinetics and metabolism of oxycodone after intramuscular and oral administration to healthy subjects. British journal of clinical pharmacology. 1992;33(6):617-21.DOI: 10.1111/j.1365-2125.1992.tb04090.x.
198. Thörn HA, Lundahl A, Schrickx JA, Dickinson PA, Lennernäs H. Drug metabolism of CYP3A4, CYP2C9 and CYP2D6 substrates in pigs and humans. Eur J Pharm Sci. 2011;43(3):89-98.DOI: 10.1016/j.ejps.2011.03.008.
199. Anzenbacher P, Soucek P, Anzenbacherová E, Gut I, Hrubý K, Svoboda Z, Květina J. Presence and activity of cytochrome P450 isoforms in minipig liver microsomes. Comparison with human liver samples. Drug metabolism and disposition: the biological fate of chemicals. 1998;26(1):56-9.DOI.
200. Nishimuta H, Nakagawa T, Nomura N, Yabuki M. Species differences in hepatic and intestinal metabolic activities for 43 human cytochrome P450 substrates between humans and rats or dogs. Xenobiotica. 2013;43(11):948-55.DOI: 10.3109/00498254.2013.787155.
201. Cecchelli R, Dehouck B, Descamps L, Fenart L, Buée-Scherrer VV, Duhem C, Lundquist S, Rentfel M, Torpier G, Dehouck MP. In vitro model for evaluating drug transport across the blood-brain barrier. Advanced drug delivery reviews. 1999;36(2-3):165-78.DOI: 10.1016/s0169-409x(98)00083-0.
202. Cooper JA, Del Vecchio PJ, Minnear FL, Burhop KE, Selig WM, Garcia JG, Malik AB. Measurement of albumin permeability across endothelial monolayers in vitro. J Appl Physiol (1985). 1987;62(3):1076-83.DOI: 10.1152/jappl.1987.62.3.1076.
203. Melander E, Eriksson C, Wellens S, Hosseini K, Fredriksson R, Gosselet F, Culot M, Göransson U, Hammarlund-Udenaes M, Loryan I. Differential Blood-Brain Barrier Transport and Cell Uptake of Cyclic Peptides In Vivo and In Vitro. Pharmaceutics. 2023;15(5).DOI: 10.3390/pharmaceutics15051507.
204. Thomsen MS, Humle N, Hede E, Moos T, Burkhart A, Thomsen LB. The blood-brain barrier studied in vitro across species. PloS one. 2021;16(3):e0236770.DOI: 10.1371/journal.pone.0236770.
205. Voirin AC, Perek N, Roche F. Inflammatory stress induced by a combination of cytokines (IL-6, IL-17, TNF-α) leads to a loss of integrity on bEnd.3 endothelial cells in vitro BBB model. Brain research. 2020;1730:146647.DOI: 10.1016/j.brainres.2020.146647.
206. Poller B, Drewe J, Krähenbühl S, Huwyler J, Gutmann H. Regulation of BCRP (ABCG2) and P-glycoprotein (ABCB1) by cytokines in a model of the human blood-brain barrier. Cellular and molecular neurobiology. 2010;30(1):63-70.DOI: 10.1007/s10571-009-9431-1.
207. Tsang YP, Hao T, Mao Q, Kelly EJ, Unadkat JD. Dysregulation of the mRNA Expression of Human Renal Drug Transporters by Proinflammatory Cytokines in Primary Human Proximal Tubular Epithelial Cells. Pharmaceutics. 2024;16(2).DOI: 10.3390/pharmaceutics16020285.
208. Le Vee M, Lecureur V, Stieger B, Fardel O. Regulation of drug transporter expression in human hepatocytes exposed to the proinflammatory cytokines tumor necrosis factor-alpha or interleukin-6. Drug metabolism and disposition: the biological fate of chemicals. 2009;37(3):685-93.DOI: 10.1124/dmd.108.023630.
209. Drakesmith H, O'Neil D, Schneider SC, Binks M, Medd P, Sercarz E, Beverley P, Chain B. In vivo priming of T cells against cryptic determinants by dendritic cells exposed to interleukin 6 and native antigen. Proc Natl Acad Sci U S A. 1998;95(25):14903-8.DOI: 10.1073/pnas.95.25.14903.

210. Chew KS, Wells RC, Moshkforoush A, Chan D, Lechtenberg KJ, Tran HL, Chow J, Kim DJ, Robles-Colmenares Y, Srivastava DB, Tong RK, Tong M, Xa K, Yang A, Zhou Y, Akkapeddi P, Annamalai L, Bajc K, Blanchette M, Cherf GM, Earr TK, Gill A, Huynh D, Joy D, Knight KN, Lac D, Leung AW, Lexa KW, Liau NPD, Becerra I, Malfavon M, McInnes J, Nguyen HN, Lozano EI, Pizzo ME, Roche E, Sacayon P, Calvert MEK, Daneman R, Dennis MS, Duque J, Gadkar K, Lewcock JW, Mahon CS, Meisner R, Solanoy H, Thorne RG, Watts RJ, Zuchero YJY, Kariolis MS. CD98hc is a target for brain delivery of biotherapeutics. Nature communications. 2023;14(1):5053.DOI: 10.1038/s41467-023-40681-4.
211. Schmitt MV, Lienau P, Fricker G, Reichel A. Quantitation of Lysosomal Trapping of Basic Lipophilic Compounds Using In Vitro Assays and In Silico Predictions Based on the Determination of the Full pH Profile of the Endo-/Lysosomal System in Rat Hepatocytes. Drug Metabolism and Disposition. 2019;47(1):49-57.DOI: 10.1124/dmd.118.084541.
212. Akino S, Yasujima T, Shibutani R, Yamashiro T, Yuasa H. Involvement of proton-coupled SLC49A4-mediated transport in the export of lysosomally trapped pyrilamine. Drug Metabolism and Disposition. 2023;52:19-25.DOI: 10.1124/dmd.123.001354.

This thesis was partially created with the assistance of GPT-4, Open AI's large-scale language generation model. I reviewed, edited, and refined the text to my own liking and retain full responsibility for the content presented in this thesis. The cover illustration was generated using GPT-4.

Biorender was used to create figures.

Acta Universitatis Upsaliensis

Digital Comprehensive Summaries of Uppsala Dissertations from the Faculty of Pharmacy 364

Editor: The Dean of the Faculty of Pharmacy

A doctoral dissertation from the Faculty of Pharmacy, Uppsala University, is usually a summary of a number of papers. A few copies of the complete dissertation are kept at major Swedish research libraries, while the summary alone is distributed internationally through the series Digital Comprehensive Summaries of Uppsala Dissertations from the Faculty of Pharmacy. (Prior to January, 2005, the series was published under the title "Comprehensive Summaries of Uppsala Dissertations from the Faculty of Pharmacy".)

Distribution: publications.uu.se
urn:nbn:se:uu:diva-540918

ACTA UNIVERSITATIS
UPSALIENSIS
2024